Bond energies of ThO^+ and ThC^+: A guided ion beam and quantum chemical investigation of the reactions of thorium cation with O_2 and CO

Richard M Cox, Murat Citir' , P. B. Armentrout' , Samuel R. Battey, and Kirk A. Peterson

Citation: J. Chem. Phys. **144**, 184309 (2016); doi: 10.1063/1.4948812
View online: http://dx.doi.org/10.1063/1.4948812
View Table of Contents: http://aip.scitation.org/toc/jcp/144/18
Published by the American Institute of Physics

Bond energies of ThO^+ and ThC^+: A guided ion beam and quantum chemical investigation of the reactions of thorium cation with O_2 and CO

Richard M Cox,[1] Murat Citir,[1,a)] P. B. Armentrout,[1,b)] Samuel R. Battey,[2] and Kirk A. Peterson[2]
[1]*Department of Chemistry, University of Utah, Salt Lake City, Utah 84112-0850, USA*
[2]*Department of Chemistry, Washington State University, Pullman, Washington 99164-4630, USA*

(Received 7 March 2016; accepted 25 April 2016; published online 13 May 2016)

Kinetic energy dependent reactions of Th^+ with O_2 and CO are studied using a guided ion beam tandem mass spectrometer. The formation of ThO^+ in the reaction of Th^+ with O_2 is observed to be exothermic and barrierless with a reaction efficiency at low energies of $k/k_{LGS} = 1.21 \pm 0.24$ similar to the efficiency observed in ion cyclotron resonance experiments. Formation of ThO^+ and ThC^+ in the reaction of Th^+ with CO is endothermic in both cases. The kinetic energy dependent cross sections for formation of these product ions were evaluated to determine 0 K bond dissociation energies (BDEs) of $D_0(Th^+–O) = 8.57 \pm 0.14$ eV and $D_0(Th^+–C) = 4.82 \pm 0.29$ eV. The present value of $D_0(Th^+–O)$ is within experimental uncertainty of previously reported experimental values, whereas this is the first report of $D_0(Th^+–C)$. Both BDEs are observed to be larger than those of their transition metal congeners, TiL^+, ZrL^+, and HfL^+ (L = O and C), believed to be a result of lanthanide contraction. Additionally, the reactions were explored by quantum chemical calculations, including a full Feller-Peterson-Dixon composite approach with correlation contributions up to coupled-cluster singles and doubles with iterative triples and quadruples (CCSDTQ) for ThC, ThC^+, ThO, and ThO^+, as well as more approximate CCSD with perturbative (triples) [CCSD(T)] calculations where a semi-empirical model was used to estimate spin-orbit energy contributions. Finally, the ThO^+ BDE is compared to other actinide (An) oxide cation BDEs and a simple model utilizing An^+ promotion energies to the reactive state is used to estimate AnO^+ and AnC^+ BDEs. For AnO^+, this model yields predictions that are typically within experimental uncertainty and performs better than density functional theory calculations presented previously. *Published by AIP Publishing.* [http://dx.doi.org/10.1063/1.4948812]

INTRODUCTION

Actinides (An) are of interest because of their use in nuclear power and because of national security concerns, however, research is hampered because of the radioactive nature of most members of the actinide series (except Th and U), which make them difficult and potentially dangerous to investigate. Therefore, it is highly desirable to employ theoretical methods to study these systems. In order to evaluate potential basis sets and theoretical methods, key fundamental experimental benchmarks are necessary. Gas-phase studies that are absent solvent effects can provide these benchmarks, and an increasing number of gas-phase studies of actinide systems have been reported.[1–17] These have been accompanied by an increasing number of theoretical reports.[14–26] Several examples of discrepancies between experimental and theoretical results exist,[14,23,24] such that this field remains in its infancy.

Of these studies, oxidation reactions are probably the best studied. Previously, Marçalo and Gibson[13] have determined that there is a correlation between bond dissociation energies (BDEs) of AnO^{p+} (p = 0–2) and the promotion energy (E_p) of An^{p+} to the lowest level having a $6d^2$ configuration (Usual ground state configurations for An are $5f^{n-3}6d7s^2$ and $5f^{n-2}7s^2$, and for An^+ are $5f^{n-2}7s^2$ and $5f^{n-1}7s$.) Th and Th^+ are unique among the actinides because they do not populate the $5f$-orbitals in their ground states having $6d^27s^2$ and $6d^27s$ ground level configurations, respectively. One interesting aspect of these configurations is that they compare directly to transition metal systems that are better understood.

Because of its $6d^27s$ ground state configuration, the E_p of Th^+ is zero and thus Th^+ is the most reactive of the actinide series and has been described as oxophilic. Because of the reactivity of the thorium cation, it is difficult to make a direct measurement of $D_0(Th^+–O)$ with thermal methods such as ion cyclotron resonance (ICR) mass spectrometry. Currently, only the lower limit $D_0(Th^+–O) \geq D_0(H_2C–O) = 7.85$ eV can be established by direct measurement on the basis of ICR results.[5] Indirectly, $D_0(Th^+–O)$ can be determined using the thermochemical cycle in

$$D_0(Th^+–O) = D_0(Th–O) + IE(Th) – IE(ThO), \quad (1)$$

where the ionization energies IE(Th) = 6.306 92 eV[9,27,28] and IE(ThO) = 6.602 63 ± 0.0002 eV[9] are well established. Evaluations of previous thermochemical data by Pedley and Marshall[29] from high temperature methods such as Knudsen

a)Present address: Abdullah Gül University, Kayseri, Melikgazi 38039, Turkey.
b)Author to whom correspondence should be addressed. Electronic mail: armentrout@chem.utah.edu

effusion experiments provide D_0(Th–O),[30–34] but such data are dependent on the free energy functions (and molecular parameters) used to adjust energies to 0 K values. Choice of parameters can have a large impact on the reported BDE,[29,32] a thorough discussion of which is presented below.

A unique aspect of guided ion beam tandem mass spectrometry (GIBMS) is the ability to control reactant energies over a large range of kinetic energies, which allows the study of the energy dependences of endothermic reactions to establish direct measurements of key thermodynamic information. Furthermore, no knowledge of product molecular parameters is needed. Accurate experimental determination of such BDEs is critical for establishing reliable benchmarks to which theoretical methods can be evaluated. Previously, MO^+ BDEs have successfully been measured using GIBMS for first,[35–38] second,[39,40] and third[41–44] row transition metals. Here we present the absolute kinetic energy dependent cross sections of the reactions of Th^+ with O_2 and CO measured using GIBMS and analyze these to determine $D_0(Th^+–O)$ and $D_0(Th^+–C)$. We also compare theoretically derived BDEs to these experimental benchmarks and discuss what implications knowledge of Th^+ thermochemical values has for the An^+ series.

Literature thermochemistry review

The thermochemistry of ThO^{n+} (n = 0, 1) is seemingly well established. Pedley and Marshall[29] reevaluated data primarily from Ackermann and Rau,[30,31] Hildenbrand and Murad,[32] and Murad and Hildenbrand[33] and established D_0(Th–O) = 9.06 ± 0.12$_5$ eV. (Pedley and Marshall cite values of 9.08 ± 0.11 eV, 9.04 ± 0.03 eV and 9.09 ± 0.15 eV,[30] 9.09 ± 0.17 eV and 9.06 ± 0.17 eV,[31] 8.97 ± 0.20 eV and 9.08 ± 0.20 eV,[32] and 9.06 ± 0.11 eV.[33]) Originally, Ackermann and Rau reported D_0(Th–O) ≤ 8.3 eV[30] in weight loss experiments and D_0(Th–O) = 9.0 ± 0.1 eV in Knudsen cell effusion experiments,[31] and Hildenbrand and Murad reported D_0(Th–O) = 8.79 ± 0.13 eV.[32] Because all data were extrapolated from high temperature regimes, both Pedley and Marshall and Hildenbrand and Murad caution that significant errors can occur in the use of free energy functions because of poorly established molecular parameters.[29,32] In this case, errors are plausible because the parameters used by Pedley and Marshall list a $^3\Delta$ first excited state with all spin-orbit (SO) levels at ~5000 cm^{-1} above the ground state (presumably on the basis of work by Edvinsson[45]). In earlier work, Huber and Herzberg[46] identify the same state as $^1\Phi$. A more recent compilation[47] of experimental data identifies the state as $^3\Delta$ but with levels found at 5317, 6128, and 8600 cm^{-1} above the ground level, which agree well with theoretical work by Paulovic *et al.*[47] and Küchle *et al.*[48]

The Gas-phase Ion and Neutral Thermochemistry (GIANT) compilation[49] references Pedley and Marshall but extrapolates to 0 K differently so that D_0(Th–O) = 9.04 ± 0.11 eV. Marçalo and Gibson later adopt the value of Pedley and Marshall, but list the uncertainty as two standard deviations of the mean, D_0(Th–O) = 9.06 ± 0.25 eV.[13] Most recently, Konings *et al.*[50] evaluated the previously reported values of the ThO BDE and concluded D_0(Th–O) = 9.00 ± 0.10 eV (we report the uncertainty as 2 standard deviations of the mean), where the Ackermann and Rau[30] values are excluded for reasons unstated and an additional value of D_0(Th–O) = 8.89 ± 0.17 eV reported by Neubert and Zmbov[34] is included. A weighted average of the values originally reported by their respective authors (9.0 ± 0.1 eV,[31] 8.79 ± 0.13 eV,[32] and 8.89 ± 0.17 eV[34]) excluding the upper limit (≤8.3 eV[30]) yields D_0(Th–O) = 8.92 ± 0.14 eV where the uncertainty is two standard deviations of the mean.

In general, reports of ThO^+ BDEs have been derived using Eq. (1). Data found in the GIANT compilation lead to a BDE of $D_0(Th^+–O)$ = 9.03 ± 0.14 eV,[49] but GIANT utilizes older values of IE(Th) = 6.08 eV[51] and IE(ThO) = 6.1 ± 0.1 eV[52] (electron ionization values). More recent spectroscopic determinations of these values are IE(Th) = 6.306 92 eV[9,27,28] and IE(ThO) = 6.602 63 ± 0.0002 eV.[9] Using the updated IEs, a value of 8.74 ± 0.14 eV can be established from the D_0(Th–O) given in the GIANT tables and Eq. (1). Marçalo and Gibson[13] report $D_0(Th^+–O)$ = 8.74 ± 0.25 eV on the basis of the Pedley and Marshall neutral BDE and the spectroscopic IEs. A value of $D_0(Th^+–O)$ = 8.70 ± 0.10 eV can be derived using Eq. (1) with the neutral BDE value reported by Konings *et al.*[50] Finally, a value of $D_0(Th^+–O)$ = 8.62 ± 0.14 eV can be derived from the weighted average of the original reports of D_0(Th–O). All values are consistent with the lower limit established in ICR studies, $D_0(Th^+–O) \geq D_0(H_2C–O)$ = 7.85 eV.[5]

Unlike ThO^{p+}, the thermochemistry of ThC^{p+} (p = 0, 1) is much less well established. The only report of the ThC BDE is D_{298}(Th–C) = 4.70 ± 0.18 eV determined in Knudsen cell effusion experiments.[53] An electron ionization energy of IE(ThC) = 7.9 ± 1.0 eV was reported in the same study and is similar to a prior value of 8.0 ± 0.1 eV.[54] Neglecting the difference between the 298 and 0 K BDEs, $D_0(Th^+–C)$ = 3.1 ± 1.0 eV can be determined using Eq. (1) and the lower IE value, a value that is probably best expressed as a lower limit for reasons discussed below.

EXPERIMENTAL AND THEORETICAL METHODS

Instrument

The GIBMS used in these experiments has been described in detail previously.[55] Briefly, ions are created in a direct current discharge/flow tube source (DC/FT) described in more detail below.[56] After exiting the source, ions are focused through a magnetic momentum analyzer where the reactant $^{232}Th^+$ ion beam is mass selected. These ions are decelerated to a well-defined kinetic energy and passed into a radio frequency (rf) octopole ion guide[57,58] that constrains the ions radially. The octopole passes through a static pressure reaction cell that contains the neutral reaction partner (O_2 or CO). To ensure that the probability of multiple collisions between Th^+ and the neutral gas is sufficiently small, the pressure in the reaction cell is maintained at typical pressures of 0.10–0.40 mTorr. Independent measurements at several pressures are performed to ensure that measured cross sections are independent of neutral reactant pressures. Reaction cross sections are calculated from product ion intensities relative to reactant ion intensities after correcting for background

ion intensities measured when the neutral gas is no longer directed into the gas cell.[59] Uncertainties in the calculated absolute cross section are estimated to be ±20%, with relative uncertainties of ±5%.

Laboratory (lab) ion energies are converted to the center-of-mass (CM) frame using the relationship $E_{CM} = E_{lab} \times m/(m + M)$ where m and M are the masses of the neutral reactant and ion, respectively. At very low energies, the conversion includes a correction for the truncation of the ion kinetic energy distribution as described previously.[59] Cross sections are known to be broadened by the kinetic energy distribution of the reactant ions and the thermal (300 K) motion of the neutral reactant.[60] The absolute zero of energy and the full width at half-maximum (fwhm) of the ion beam are determined by using the octopole guide as a retarding potential analyzer.[59] Typical fwhms of the energy distribution for these experiments were 0.4–0.6 eV (lab). Uncertainties in the absolute energy scale are 0.1 eV (lab). All energies reported below are in the CM frame.

Ion source

The DC/FT source has been described in detail previously.[56] Briefly, a cathode containing the thorium powder sample (^{232}Th, 100% abundance) is held at ∼2.5 kV. The resultant electric field ionizes Ar gas that flows over the cathode in a 9:1 He/Ar mixture. The ionized Ar collides with the cathode and Th^+ ions are sputtered off and swept into the flow tube by the He/Ar flow at typical pressures of 0.3–0.4 Torr. In the flow tube, ions thermalize by $\sim 10^5$ collisions with carrier gas. In this work and previous work with Th^+,[16,17] there is no evidence of excited state species. Previous experiments[61–65] utilizing the DC/FT source with transition metal ions have indicated that the internal of temperature of ions generated is 300–1100 K. A population analysis at 300 K indicates that 99.89% of Th^+ is in its ground level ($^4F_{3/2}$, $6d^27s$), whereas at 1100 K, 76% is in the ground level.[28,66] Conservatively, we estimate the internal temperature to be 700 ± 400 K, where Th^+ has an average electronic energy of $E_{el} = 0.02 \pm 0.03$ eV. The average excitation energy and its uncertainty are incorporated into all threshold and bond dissociation energies reported here.

Data analysis

The kinetic energy dependence of endothermic reactions is modeled using[58,67,68]

$$\sigma(E) = \sigma_0 \Sigma g_i (E + E_{el} + E_i - E_0)^n / E, \quad (2)$$

where σ_0 is an energy-independent scaling factor, E is the relative kinetic energy of the reactants, E_i is the internal energy of the neutral reactants having populations g_i ($\Sigma g_i = 1$), n is an adjustable parameter, and E_0 is the 0 K reaction threshold. Before comparison to the data, Eq. (2) is convoluted over the kinetic energy distributions of the reactants, and the σ_0, n, and E_0 parameters are optimized using a nonlinear least-squares method to best reproduce the experimental cross section.[59,69] Uncertainties in E_0 are calculated from the threshold values from several independent data sets over a range of acceptable n values and combined with the absolute uncertainties in the kinetic energy scale and internal energies of reactant ions (0.02 ± 0.03 eV). At high energies, cross sections decline because of product dissociation, so Eq. (2) is modified to include a statistical model of the dissociation probability, as discussed in detail elsewhere.[70] Briefly the dissociation probability is controlled by two adjustable parameters: p, which is similar to n, can hold only integer values and E_d, the energy at which product cross sections begin to decline. In most cases, inclusion of the high-energy model does not significantly alter the analysis of E_0, however, when a significant deviation is observed, the model that most accurately reproduces the experimental cross section in the threshold region is used. Consequently, for $Th^+ + CO \rightarrow ThO^+ + C$, the high energy model is not included in the present threshold analysis.

E_0 obtained from Eq. (2) is used to determine the bond dissociation energy (BDE), $D_0(Th^+–L)$, using Eq. (3) where L = O or C

$$D_0(Th^+–L) = D_0(CO)–E_0, \quad (3)$$

Eq. (3) assumes that there are no barriers in excess of the endothermicity of the reaction. No experimental evidence was found to suggest that such a barrier is present in either system studied here, and potential energy surfaces (PESs) presented below confirm that no barriers are present.

Theoretical calculations

The majority of the quantum chemical calculations were performed using the Gaussian 09 suite of programs.[71] For Th^+, a polarized correlation consistent core-valence quadruple-ζ (20s17p12d11f7g4h1i)/[9s9p8d8f7g4h1i] basis set[72] was used with the Stuttgart-Cologne multiconfigurational Dirac Hartree-Fock (MDF) small core (60 electron) relativistic effective core potential[73] (ECP), cc-pwCVQZ-PP. The cc-pwCVTZ-PP[72] and atomic natural orbital ANO-VQZ-MDF[73] basis sets were also used in combination with the MDF ECP. Additionally, Stuttgart-Dresden (SDD-VDZ-MWB), segmented quadruple-ζ (Seg. SDD-VQZ-MWB), and atomic natural orbital (ANO-VQZ-MWB) basis sets[48,74] were used in combination with the Stuttgart-Dresden small core quasi-relativistic ECP (MWB). The aug-cc-pwCVQZ,[75] cc-pwCVXZ (X = T, Q),[76] and Pople[77] 6-311+ G(3df) basis set were used for C and O. Extrapolation to the complete basis set (CBS) limit for the cc-pwCVXZ (X = T, Q) basis sets was performed using the Karton-Martin method,[78] Eq. (4), for Hartree Fock (HF) energies (where Y = 3 for T and Y = 4 for Q)

$$E_X = E_{CBS} + A(Y + 1)e^{-6.57\sqrt{Y}}. \quad (4)$$

For coupled-cluster singles and doubles with perturbative (triples) [CCSD(T)]/cc-pwCVXZ calculations, Eq. (5)[79] is used to extrapolate the correlation energy

$$E_X = E_{CBS} + B(Y + 1/2)^{-4}. \quad (5)$$

The use of these basis sets has previously yielded reasonable results for other Th^+ and Th systems.[16,17,72,80–82]

Structures were optimized using density functional theory functionals, B3LYP,[83,84] B3PW91,[85] BH and HLYP (BH-LYP),[86] M06,[87] and PBE0[88] with unrestricted wavefunctions.

B3LYP and B3PW91 have proven reliable in actinide theoretical calculations by us and others.[16,17,20,24] PBE0 and M06 have also yielded reasonable results and M06 was indicated as a promising functional in studies of the ThO_2^+ BDE.[17,26] BHLYP has previously performed well in actinide systems when the molecule is singly bound[16,17] but performs poorly in systems with higher bond orders.[16,89] Nevertheless, it is included here because it appears to perform well in energy spacing between electronic states in previous studies of Th^+.[16,17] Additionally, single point energies using a spin unrestricted coupled cluster method that mixes in single and double excitations and perturbative triple excitations, CCSD(T),[90–93] are performed using the B3LYP optimized structures. For electron correlation calculations using CCSD(T), the Th^+ 5*s* and 5*p* and the C/O 1*s* electrons are frozen. All energies discussed below are corrected by the zero point energy using the frequencies generated at their respective optimized structure after scaling by 0.989.[94] Potential energy surfaces are generated by performing relaxed potential scans along the ∠LThO$^+$ coordinate (L = C or O).

For the above theoretically calculated BDEs, a semi-empirical approach that corrects for spin-orbit (SO) splitting is employed. This model is described in detail elsewhere.[16,43,44,95,96] Briefly, the uncorrected theoretical BDE is a value averaged over all spin-orbit states of the molecule and the dissociation asymptote. To correct for the SO splitting of the asymptote, the contributions of L are considered negligible, and contributions of Th^+ are corrected by the difference in energy of the ground level and the energy of the ground state averaged over all SO levels. For Th^+, the J = 3/2 ground level is a mixture of the $^4F_{3/2}$ and $^2D_{3/2}$ levels. For the purpose of comparing experimental energies to theoretical energies, we have previously assigned the ground level as $^4F_{3/2}$.[16] Experimentally, the $^4F_{3/2}$ ground level lies 0.40 eV below the SO averaged ^{2}D ground state, which lies 0.06 eV below the SO averaged ^{4}F state. The SO energy of ThL^+ can be corrected using a model described elsewhere,[16,43,44,95,96] however, for the present systems, ThL^+ ground states are Σ states (as discussed below) that do not exhibit first-order SO splitting, such that no additional correction is necessary, although this ignores any potential second-order effects from interacting states. For the present systems, potential interacting states are separated sufficiently in energy that second-order effects are not believed to be significant. Furthermore, the empirical spin-orbit correction used here is comparable to the spin-orbit contributions calculated using a composite thermochemistry approach described below.

Composite thermochemistry with explicit spin-orbit calculations

Accurate composite thermochemistry, as outlined in the Feller-Peterson-Dixon (FPD) method,[97,98] was used to describe the numerous contributions to the atomization energies at 0 and 298 K for ThC^+, ThC, ThO^+, and ThO. The majority of these calculations were carried out at the CCSD(T) level of theory with the third order Douglas-Kroll-Hess (DKH3) Hamiltonian[99,100] utilizing aug-cc-pVXZ-DK basis sets[76,101,102] on the O and C atoms and the all-electron cc-pVXZ-DK3 basis sets on Th (X = D, T, Q)[72] (denoted cc-pVXZ-DK3 below). Core-valence correlation (1*s* on C and O with 5*s*5*p*5*d* on Th) was also considered, and in these cases, the aug-cc-pwCVXZ-DK (O, C)[103] and cc-pwCVXZ-DK3 (Th)[72] basis sets were used. Geometries were optimized at the CCSD(T)/cc-pVQZ-DK3 level of theory and were consistently used as the reference geometries for all single point calculations except in the case of the zero point energy (ZPE) described below. Open-shell calculations employed restricted open-shell HF (ROHF) orbitals but the spin restriction was relaxed in the CCSD(T) calculations, i.e., the R/UCCSD(T) method[104–106] was used. Because of the highly multi-reference character of the $^4F_{3/2}$ ground state of Th^+ when SO is included, all dissociation energy calculations below were carried out relative to the ground electronic state of neutral Th atom ($^3F_2$). The calculated dissociation energies were then corrected to the ground state of the Th^+ cation using the accurate experimental ionization energy (IE) of Th atom (50 868.71(8) cm^{-1} or 6.306 92(1) eV).[9] All of these calculations, excluding the SO contributions, were carried out using the MOLPRO quantum chemistry package.[107]

The final FPD calculated dissociation enthalpies at 0 K consisted of the following contributions:

$$D_0 = E_{VQZ-DK} + \Delta E_{CBS} + \Delta E_{CV} + \Delta E_{SO} + \Delta E_{QED} + \Delta E_T + \Delta E_Q + \Delta E_{IE} + \Delta E_{ZPE}, \quad (6)$$

where E_{VQZ-DK} is the equilibrium dissociation energy at the frozen-core CCSD(T)/cc-pVQZ-DK3 level of theory. The HF energies were then extrapolated to the CBS limit using Eq. (4) with cc-pVTZ-DK3 and cc-pVQZ-DK3 basis sets, while the correlation energies were extrapolated to their CBS limits using Eq. (5). The results of these two extrapolations for the molecules and atoms were combined to yield the total CBS limit dissociation energies, with the difference between the latter values and E_{VQZ-DK} yielding ΔE_{CBS}. ΔE_{CV} is the core correlation contribution, $E_{CV} - E_{valence}$, both in the same cc-pwCVXZ-DK3 basis sets (X = T and Q), extrapolated to the CBS limit using Eq. (4). The value of E_{CV} was obtained by correlating the 5s, 5p, and 5d electrons of Th and the 1s electrons of C and O in addition to the valence electrons.

SO contributions, ΔE_{SO}, were calculated using the exact two-component (X2C) Hamiltonian[108,109] with uncontracted cc-pVDZ-DK3 basis sets and 2-component open-shell coupled cluster, CCSD(T),[109] for Th, ThC^+, ThO, ThO^+ and Fock space CCSD (FS-CCSD)[110] for ThC. The open-shell calculations for the Th atom utilized average-of-configuration HF orbitals (1 electron in the 10 spinors arising from the 6d orbitals). All SO calculations involving coupled cluster correlated only the valence electrons and were carried out using a virtual orbital cutoff of 12.0 a.u. The FS-CCSD calculations on ThC involved calculating the (0,2) sector from the closed-shell ThC^{2+} reference state. Analogous calculations were also carried out for ThC^+ [from sector (0,1)] in order to obtain a consistent SO correction for the ionization energy of ThC. The SO calculations were carried out using the DIRAC program.[111] The SO contributions for the O and C atoms (0.009 67 and 0.003 67 eV, respectively) were obtained from their experimental energy levels.[112]

ΔE_{QED} is a contribution for quantum electrodynamic (QED) effects, namely, the Lamb shift. When considering molecules that contain heavy atoms such as actinides, this contribution can begin to become significant.[113] In this work, the local potential approach of Pyykkö has been used for both the vacuum polarization and self-energy contributions.[72,114] The latter were carried out with the MOLPRO program at the frozen-core CCSD(T) level of theory with the cc-pwCVDZ-DK3 basis sets at the frozen-core cc-pVQZ-DK3 geometries.

The next two terms, ΔE_T and ΔE_Q, account for valence electron correlation effects beyond the CCSD(T) level of theory. The ΔE_T term is defined as the difference between CCSD with iterative triples (CCSDT)[115–117] and CCSD(T) in the cc-pVTZ-DK3 basis set. The effects of quadruple excitations, ΔE_Q, were defined as the difference between coupled-cluster singles and doubles with iterative triples and quadruples (CCSDTQ)[118–121] and CCSDT using cc-pVDZ-DK3 basis sets. The CCSDTQ/cc-pVDZ-DK3 calculations on ThO involved just under 4.3×10^9 configurations. The MRCC program[122] as interfaced to MOLPRO was used for all the higher-order electron correlation calculations. After correcting the dissociation energies of ThC^+ and ThO^+ to the Th^+ dissociation asymptote using the experimental IE of Th,[9] ΔE_{IE}, harmonic frequencies at the frozen-core CCSD(T)/cc-pVDZ-DK3 level of theory were used to define the zero point vibrational energy of each molecule, yielding ΔE_{ZPE}. Thermal corrections, $\Delta H_{(0-298)}$, were calculated using standard ideal gas partition functions to adjust the 0 K dissociation energies to 298 K, i.e., $D_{298} = D_0 - \Delta H_{(0-298)}$.

EXPERIMENTAL RESULTS

$Th^+ + O_2$

The cross sections as a function of kinetic energy for the reaction of thorium cation with molecular oxygen at a pressure of 0.3 mTorr are presented in Figure 1. The following reactions were observed:

$$Th^+ + O_2 \rightarrow ThO^+ + O, \quad (7)$$

$$ThO^+ + O_2 \rightarrow ThO_2^+ + O. \quad (8)$$

The energy dependence of the cross section for reaction (7) declines with increasing energy, consistent with an exothermic, barrierless reaction. At low energies, the reaction efficiency is $k/k_{LGS} = 1.21 \pm 0.24$, where the collision limit, k_{LGS}, is the Langevin-Gioumousis-Stevenson (LGS) formula.[123] This result is consistent with the results of two separate FT-ICR studies where the reaction efficiency was observed as $k/k_{LGS} = 1.12 \pm 0.22$[3] and $k/k_{LGS} = 0.86 \pm 0.43$.[5] The cross section declines with an energy dependence of $E^{-0.40\pm0.1}$, consistent with the energy dependence ($E^{-1/2}$) of the LGS cross section (σ_{LGS}) until approximately 0.6 eV where the cross section levels until 2 eV. At 2 eV, the cross section begins to decline more rapidly until dropping off even faster beginning near 6 eV. The rapid decline starting near 6 eV can be attributed to there being sufficient energy present to dissociate the ThO^+ product, a process that can begin at $D_0(O–O) = 5.117$ eV.[124]

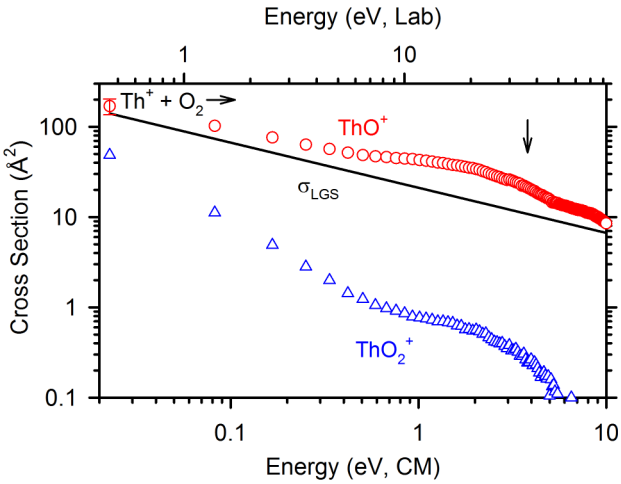

FIG. 1. The absolute cross section for the reaction of $Th^+ + O_2$ as a function of kinetic energy in the laboratory (upper x-axis) and center-of-mass (lower x-axis) frames. The solid line represents the Langevin-Giomousis-Stevenson collision limit. The arrow shows $D_0(O–O) = 5.117$ eV.

The energy dependence of reaction (7) from 0.6 to 2 eV is unusual because the cross section deviates from σ_{LGS} and has a shallower energy dependence. This energy dependence cannot be a transition to the hard sphere collision limit, which we estimate as 16 Å^2 calculated using the atomic radii reported by Waber and Cromer[125] (Th = 1.186 Å and O = 0.450 Å) and r(O–O) = 1.208 Å reported by Huber and Herzberg.[126] (Note that the atomic radius is used as an estimate of the Th^+ ionic radius, but the expected error will be minimal.) A similar energy dependence has been observed previously in the reactions of Zr^+ and Nb^+ with O_2.[40] A possible explanation, explored and previously presented in detail,[40] is that these reactions couple with the $M^{2+} + O_2^-$ asymptote thus creating a Coulombic interaction ($V_1 \propto r^{-1}$) that is more attractive than the ion–induced dipole interaction ($V_4 \propto r^{-4}$). In the Zr^+ and Nb^+ cases, the $M^{2+} + O_2^-$ asymptotes are too high in energy to influence the reaction dynamics.[40] By contrast, the deviation from σ_{LGS} occurs at higher energies for Th^+ and $IE(Th^+) = 11.65 \pm 0.35$ eV[13] is significantly smaller than $IE(Zr^+) = 13.1$ eV and $IE(Nb^+) = 14.0$ eV.[28] Thus, the Coulombic interaction may be significant in the Th^+ case. Calculations of the V_1 and V_4 surfaces following the procedure in Ref. 40 are explained in detail in the supplementary material.[129] These results indicate that near 0.5 eV, the distance r at the $V_1 = V_4$ crossing point exceeds the r value at the maximum along the V_4 surface that defines the LGS cross section. Consequently, the reaction may crossover and proceed along the more attractive V_1 potential at larger intermolecular distances, yielding a larger cross section.

The ThO_2^+ cross section in Figure 1 is dependent on the O_2 neutral reactant gas pressure, indicating that ThO_2^+ forms in a sequential process, reaction (8). The cross section for reaction (8) has an energy dependence of $E^{-1.1\pm0.2}$, consistent with that expected for product formation in sequential reactions occurring at the LGS rate. The observation of reaction (8) is interesting because direct measures of the reaction $ThO^+ + O_2$ yield no products in FT-ICR experiments at thermal energies.[3,12] Consistent with these ICR observations, GIBMS studies of the $ThO^+ + O_2$ reaction in our lab yield

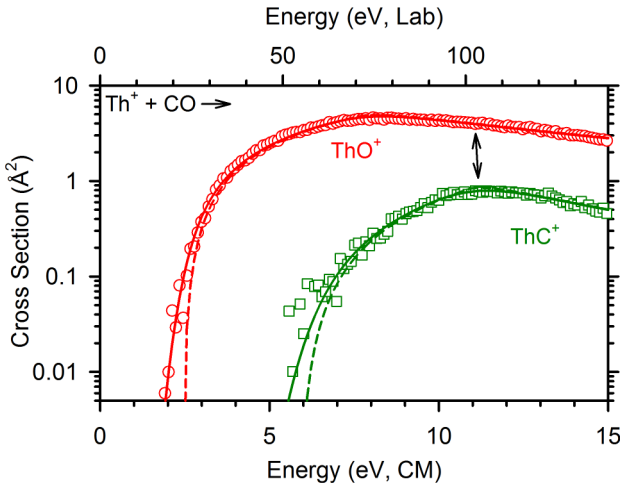

FIG. 2. The absolute cross section for the reaction of $Th^+ + CO$ as a function of kinetic energy in the laboratory (upper x-axis) and center-of-mass (lower x-axis) frames with model cross sections, Eq. (2), convoluted over the reactant internal and kinetic energy distributions (solid lines) and unconvoluted (dashed lines). The arrow shows $D_0(C–O) = 11.109$ eV.

an energy dependence inconsistent with a simple exothermic reaction. Because of these unusual reaction dynamics, a more complete analysis of this reaction is beyond the scope of the present text and will be published elsewhere.[127] Ultimately, the explanation for this dichotomy is that reaction (8) is observed because the ThO^+ products from reaction (7) are not thermalized.

$Th^+ + CO$

The cross sections of the reaction of Th^+ with CO as a function of kinetic energy are presented in Figure 2. Both reactions 9 and 10 are observed,

$$Th^+ + CO \rightarrow ThO^+ + C, \quad (9)$$

$$\rightarrow ThC^+ + O. \quad (10)$$

Reaction (9) has an apparent threshold of 2.5 eV with a cross section that increases with increasing energy until it peaks near 8 eV. Reaction (10) has an apparent threshold near 7.5 eV that corresponds with the initial decline of the ThO^+ cross section. The ThC^+ cross section peaks near $D_0(C–O) = 11.109 \pm 0.005$ eV.[124] Although not apparent on the logarithmic scale on Figure 2, the total $Th^+ + CO$ reaction cross section peaks near $D_0(C–O)$ where sufficient energy is available to allow both ThO^+ and ThC^+ product to dissociate, equivalent to atomizing CO according to reaction 11,

$$Th^+ + CO \rightarrow Th^+ + O + C. \quad (11)$$

THERMOCHEMICAL AND THEORETICAL RESULTS

ThO^+

The barrierless cross section for reaction (7) indicates that $D_0(Th^+–O) \geq D_0(O–O) = 5.117 \pm 0.001$ eV, consistent with previous ICR results[3,5] and reported literature values.[13,50] Modelling the ThO^+ cross section of reaction (9) reproduces the experimental cross section over the entire energy range, Figure 2. The measured threshold is $E_0 = 2.54 \pm 0.14$ eV

TABLE I. Fitting parameters from Eq. (1) for the indicated reaction cross section.

Reaction	n	σ_0	E_0 (eV)	$D_0(Th^+–L)$
$Th^+ + CO \rightarrow ThO^+ + C$	1.4 ± 0.2	3.5 ± 1.0	2.54 ± 0.14	8.57 ± 0.14
$Th^+ + CO \rightarrow ThC^+ + O$	1.6 ± 0.2	0.8 ± 0.3	6.29 ± 0.29	4.82 ± 0.29

with other modelling parameters used in Eq. (2) listed in Table I. This yields $D_0(Th^+–O) = 8.57 \pm 0.14$ eV from Eq. (3). The present value is lower than (but within experimental uncertainty of) the BDE adopted by Marçalo and Gibson, 8.74 ± 0.25 eV,[13] and is within combined experimental uncertainties of the value derived from Konings *et al.*, 8.70 ± 0.10 eV.[50] Interestingly, when combined with IE(Th) and IE(ThO) in Eq. (1), the present value leads to $D_0(Th–O) = 8.81 \pm 0.16$ eV, which agrees very well with $D_0(Th–O) = 8.79 \pm 0.13$ eV, originally reported by Hildenbrand and Murad,[32] and with $D_0(Th–O) = 8.89 \pm 0.17$ eV originally reported by Neubert and Zmbov.[34] Thus, the present work suggests that the lower values of $D_0(Th–O)$ in the literature are probably more accurate.

The ground and excited states of ThO^+ calculated with the cc-pwCVQZ-PP basis sets are listed in Table II. Values obtained using additional basis sets are listed in Table S1 in the supplementary material.[129] The calculated ground state of ThO^+ is $^2\Sigma^+$ with a $(1\sigma)^2(2\sigma)^2(1\pi)^4(3\sigma)^1$ molecular orbital occupation. The 1σ-orbital is the O 2*s*-orbital, the 2σ-bonding orbital is formed as two O $2p_z$-electrons are donated into an empty Th^+ $6d_{z^2}$-orbital, and the 1π-bonding orbitals are formed as the remaining O 2*p*-electrons pair with the two Th^+ $6d\pi$-electrons. Note that this configuration corresponds to a triple bond, consistent with the very strong bond. The radical electron is found in the 3σ-orbital, which is largely composed of the Th^+ 7*s*-orbital, indicating that the $^2\Sigma^+$ state forms from the atomic asymptote, Th^+ (^{4}F, $6d^27s$) + O (^{3}P), the ground level configuration. A natural bond orbital (NBO) analysis using the B3LYP/cc-pwCVQZ-PP-MDF/aug-cc-pwCVQZ approach is listed in Table S2 and verifies this bonding model. Previous theoretical reports also find a $^2\Sigma^+$ ground state with the singly occupied σ-orbital having 93% 7*s*-character.[22,26] A low-lying $^2\Delta$ state is also found 0.35–0.58 eV higher in energy than the ground state where the lone electron moves to a $6d\delta$-orbital (1δ molecular orbital). A relaxed potential scan of the diabatic potential energy surface for dissociation of ThO^+ ($^2\Delta$), Figure S2, suggests that the $^2\Delta$ state correlates with the Th^+ (^{4}F, $6d^3$) + O (^{3}P) asymptote. A third doublet state ($^2\Pi$) where an electron from the $1\pi_b$ bonding orbital is moved to the Th^+ 7*s*-orbital, $(1\sigma)^2(2\sigma)^2(1\pi)^3(3\sigma)^2$, is also found 0.73–1.22 eV higher in energy and is most likely formed from Th^+ (^{2}D, $6d7s^2$) + O (^{3}P). Because the J = 3/2 level has $^4F_{3/2}$ and $^2D_{3/2}$ mixed character, the $^2\Pi$ state presumably can form directly from the Th^+ ground level. Additional states were also found but were at least 4 eV higher in energy, Table II.

Experiments performed using pulsed field ionization-zero kinetic energy (PFI-ZEKE) photoelectron spectroscopy have determined a $^2\Sigma^+$ ground state for ThO^+.[9] Low-lying levels of $^2\Delta_{3/2}$, $^2\Delta_{5/2}$, and $^2\Pi_{1/2}$ at 0.36, 0.72, and 0.92 eV, respectively, above the ground state were also found. For reference to the

TABLE II. Molecular parameters and relative energies (in eV) of low lying states of ThO^+ and ThC^+.[a]

ThL^+	State	r(Th^+–L)[b]	ν[b]	Expt.[c]	CCSD(T)[d]	B3LYP	B3PW91	BHLYP	M06	PBE0
ThO^+	$^2\Sigma^+$ ($1\sigma^2 2\sigma^2 1\pi^4 3\sigma$)	1.808(1.807)	950(955)	0.00	0.00	0.00	0.00	0.00	0.00	0.00
	$^2\Delta$ ($1\sigma^2 2\sigma^2 1\pi^4 1\delta$)	1.825	902(918[e])	0.58[f]	0.58	0.51	0.41	0.48	0.36	0.41
	$^2\Pi$ ($1\sigma^2 2\sigma^2 1\pi^3 3\sigma^2$)	1.834	884(904)	0.92[g]	1.21	0.96	0.84	1.01	0.73	0.86
	$^4\Delta$ ($1\sigma^2 2\sigma 1\pi^4 1\delta 3\sigma$)	2.003	672		4.48	4.25	4.24	3.95	4.56	4.21
	$^4\Pi$ ($1\sigma^2 2\sigma 1\pi^4 3\sigma 2\pi$)	2.007	666		4.91	4.39	4.42	4.20	4.57	4.41
	$^4\Sigma^+$ ($1\sigma^2 2\sigma 1\pi^4 3\sigma 4\sigma$)	2.006	669		5.07	4.49	4.52	4.33	4.70	4.52
	$^4\Sigma^-$ ($1\sigma^2 2\sigma 1\pi^4 1\delta^2$)	2.017	653		5.35	5.20	5.13	4.87	5.36	5.09
ThC^+	$^2\Sigma^+$ ($1\sigma^2 1\pi^4 2\sigma$)	1.902	903		0.00	0.00	0.00	0.00	0.00	0.00
	$^4\Pi$ ($1\sigma^2 1\pi^3 2\sigma 3\sigma$)	2.049	766		0.80	0.61	0.69	0.52	0.94	0.70
	$^2\Pi$ ($1\sigma^2 1\pi^3 2\sigma^2$)	2.023	668		0.82	0.64	0.77	0.55	0.85	0.77
	$^4\Phi$ ($1\sigma^2 1\pi^3 2\sigma 1\delta$)	2.068	737		1.32	1.07	1.09	0.95	1.22	1.09
	$^4\Sigma^-$ ($1\sigma^2 1\pi^2 2\sigma^2 1\delta$)	2.124	696		1.55	1.31	1.46	1.27	1.50	1.50
	$^2\Delta$ ($1\sigma^2 1\pi^4 1\delta$)	1.962	828		1.79	1.68	1.76	1.68	1.67	1.79
	$^2\Pi$ ($1\sigma^2 1\pi^4 2\pi$)	1.970	814		2.41	2.08	2.12	2.17	2.02	2.18

[a]Structure optimized at respective level of theory (except CCSD(T)) using cc-pVQZ-PP/6-311+G(3df) basis sets.
[b]Bond lengths (in Å) or frequencies (in cm^{-1}) from B3LYP/cc-pVQZ-PP/6-311+G(3df) optimized structures. Frequencies scaled by 0.989. Values in parentheses are experimental values from Ref. 9.
[c]Reference 9.
[d]Single point energies calculated using B3LYP/cc-pVQZ-PP/6-311+G(3df) optimized structures.
[e]Frequency of the $^2\Delta_{3/2}$ level. Frequency of the $^2\Delta_{5/2}$ level is 915 cm^{-1}.
[f]Average energy of the $^2\Delta$ state weighted over all spin-orbit degeneracies.
[g]Energy of the $^2\Pi_{1/2}$ level.

theoretical values, which are an average energy of all SO levels, the experimental average of the $^2\Delta$ levels weighted over the SO degeneracies is 0.58 eV. Table II indicates that the present calculations are in very good agreement with the experimental electronic state energies.

Bond lengths and vibrational frequencies calculated using B3LYP/cc-pwCVQZ-PP/aug-cc-pwCVQZ are listed in Table II. Molecular parameters calculated using additional levels of theory are listed in Tables S3 and S4 in the supplementary material.[129] In general, the B3LYP/cc-pwCVQZ-PP/aug-cc-pwCVQZ values agree very well with the experimental values. This is particularly true for the $^2\Sigma^+$ ground state where theory is in very good agreement with the experimental bond length, 1.808 Å,[9] and the calculated frequency differs from experiment by only 5 cm^{-1}.

The breakdown of the contributions to the FPD dissociation energies of ThC^+, ThC, ThO^+, and ThO is shown in Table III. Among the CCSD(T) contributions, the CBS extrapolations increased the cc-pVQZ-DK3 dissociation energies by about 5.8–6.7 kJ/mol, whereas core-valence correlation provided further increases of 10–13 kJ/mol for the oxides. The effects of electron correlation beyond CCSD(T) were a bit surprising. The difference between full iterative and perturbative triples was about −5 kJ/mol in all four cases (decreasing the CCSD(T) D_e values), but the contributions of connected quadruples were relatively small, only about ±1.2 kJ/mol for the two cations and about +2.0 and +0.3 kJ/mol for ThC and ThO, respectively. As expected, the spin-orbit contributions mostly result from the atomic splitting in Th atom and range from −38 to −44 kJ/mol. After inclusion of the Th/Th^+ correction for ThC^+ and ThO^+, as well as the ZPE corrections of 5.0–5.4 kJ/mol, the final 0 K BDEs are calculated to be 5.00 (ThC^+), 4.97 (ThC), 8.68 (ThO^+), and 8.98 (ThO) eV, respectively. Given the magnitude of the

TABLE III. Calculated contributions to the dissociation energies within the FPD scheme in kJ/mol (eV). See Eq. (6) for details.

Molecule	E_{VQZ-DK}	ΔE_{CBS}	ΔE_{CV}	ΔE_{QED}	ΔE_T	ΔE_Q	ΔE_{SO}	ΔE_{IE}	ΔE_{ZPE}	D_0	D_{298}
ThC^+	−88.89	+6.56	+1.37	+3.52	−5.04	+1.22	−40.02	608.53	−4.94	482.30	485.89
($^2\Sigma^+$)[a]	(−0.92)	(+0.07)	(+0.01)	(+0.04)	(−0.05)	(+0.01)	(−0.41)	(6.31)	(−0.05)	(5.00)	(5.04)
ThC	517.86	+7.22	+5.31	+1.95	−5.79	+1.80	−44.05	N/A	−4.80	479.51	483.35
($^3\Sigma^+$)[b]	(5.37)	(+0.07)	(+0.06)	(+0.02)	(−0.06)	(+0.02)	(−0.46)		(−0.05)	(4.97)	(5.01)
ThO^+	264.13	+5.79	+10.59	+1.41	−5.05	−1.09	−41.00	608.53	−5.49	837.81	841.92
($^2\Sigma^+$)[c]	(2.74)	(+0.06)	(+0.11)	(+0.01)	(−0.05)	(−0.01)	(−0.42)	(6.31)	(−0.06)	(8.68)	(8.73)
ThO	894.82	+6.56	+12.84	+0.11	−5.13	+0.30	−37.89	N/A	−5.14	866.47[e]	870.55
($^1\Sigma^+$)[d]	(9.27)	(+0.07)	(+0.13)	(+0.00)	(−0.05)	(+0.00)	(−0.39)		(−0.05)	(8.98)	(9.02)

[a]At a FC-CCSD(T)/cc-pVQZ-DK3 equilibrium bond length of 1.9269 Å. Combining the current results for ThC^+ and ThC yields a final FPD ionization energy at 0 K of 610.22 kJ/mol (6.24 eV).
[b]At a FC-CCSD(T)/cc-pVQZ-DK3 equilibrium bond length of 1.9617 Å.
[c]At a FC-CCSD(T)/cc-pVQZ-DK3 equilibrium bond length of 1.8127 Å. Combining the current results for ThO^+ and ThO yields a final FPD ionization energy at 0 K of 637.18 kJ/mol (6.60 eV) compared to the experimental value[9] of 637.0570(25) kJ/mol.
[d]At a FC-CCSD(T)/cc-pVQZ-DK3 equilibrium bond length of 1.8488 Å.
[e]Using the experimental IEs of both ThO and Th atom, this yields a D_0 for ThO^+ of 837.93 kJ/mol (8.68 eV).

TABLE IV. Comparison of theoretical $D_0(Th^+–L)$ to experimental values (in eV).[a]

	Experimental			Theoretical			
ThL^+	Literature	This work	Basis set	CCSD(T)[b]	B3LYP	B3PW91	PBE0
ThO^+	8.74 ± 0.25[c]	8.57 ± 0.14	SDD	8.76	8.61	8.73	
	8.70 ± 0.10[d]		Seg. SDD	8.55	8.75	8.88	8.82
	≥7.85[e]		cc-pwCVQZ-PP[f]	8.70	8.70	8.80	8.75
			CBS-PP[g]	8.94	8.89	8.99	8.94
			FPD[h]	8.68			
ThC^+	≥3.12 ± 0.21[i]	4.82 ± 0.29	SDD	4.90	4.84	5.21	
			Seg. SDD	4.72	4.92	5.30	5.33
			cc-pwCVQZ-PP	4.92	4.81	5.16	5.20
			CBS-PP	5.18	4.99	5.34	5.38
			FPD[h]	5.00			
MAD[j]			SDD	0.14	0.03	0.28	
			Seg. SDD	0.06	0.14	0.40	0.38
			cc-pwCVQZ-PP	0.11	0.07	0.29	0.28
			CBS-PP	0.36	0.25	0.47	0.46
			FPD	0.15			

[a]From structures optimized at the respective level of theory (except CCSD(T)) with the indicated basis set. Energies include estimated spin-orbit correction of −0.40 eV. See text and Ref. 16.
[b]Energies from single point calculations using B3LYP optimized structures with the indicated basis set for Th^+.
[c]Reference 13.
[d]Calculated from D_0(Th–O) from Ref. 50 utilizing IE(ThO) from Ref. 9 and IE(Th) from Ref. 28. See text.
[e]Reference 5.
[f]cc-pwCVQZ-PP/aug-cc-pwcVQZ basis sets.
[g]Complete basis set limit extrapolated from pwCVXZ-PP/cc-pwCVXZ (X = T, Q) basis sets using Eqs. (4) and (5), see text.
[h]Feller-Peterson-Dixon model for composite thermochemistry. See text and Eq. (6). See Table III.
[i]Reference 53.
[j]Mean absolute deviation from experimental value.

higher order correlation contributions, as well as the other terms, these dissociation energies are expected to be accurate to within about 0.05 eV.

All of the theoretical BDEs for ThO^+ calculated in this work are presented in Table IV. After inclusion of spin-orbit effects, theoretical BDEs are 8.61–8.76, 8.55–8.88, 8.70–8.80, and 8.89–8.99 eV for the SDD-VDZ-MWB, Seg. SDD-VQZ-MWB, and cc-pwCVQZ-PP/aug-cc-pwCVQZ basis sets, and CBS limit, respectively. Likewise the FPD composite thermochemistry approach yields a BDE of 8.68 eV. BDEs calculated with additional basis sets and methods are listed in Table S5 in the supplementary material.[129] In general, B3LYP and CCSD(T) values (except CCSD(T)/CBS) are in good agreement with the experimental BDE reported here. Previous work by Pereira *et al.*[14] has calculated theoretical BDEs for ThO^+ using the Seg. SDD-VQZ-MWB basis set for Th^+ and a 10*s*6*p* basis contracted to 5*s*3*p* by Dunning for O in conjunction with B3LYP and MPW1PW91 DFT functionals. They find $D_0(Th^+–O)$ of 9.02 and 9.29 eV for B3LYP and MPW91PW91 approaches, respectively, with no consideration for spin-orbit energy. Applying the spin-orbit correction used here yields values of 8.62 and 8.89 eV, respectively, where the B3LYP value is in very good agreement with the present experimental work.

ThC^+

Modeling of the cross section from reaction (10) indicates that $E_0 = 6.29 \pm 0.29$ eV, leading to $D_0(Th^+–C) = 4.82 \pm 0.29$ eV. (Note that the large uncertainty compared to the ThO^+ BDE results from the smaller overall cross section, which leads to a lower signal-to-noise ratio.) To the best of our knowledge, no determination of the ThC^+ BDE has been reported in the literature, although the value, $D_0(Th^+–C) = 3.1 \pm 1.0$ eV, can be calculated from Eq. (1) using data from Knudsen cell experiments.[53] For reasons discussed below, the latter value is almost certainly too low because IE(ThC) = 7.9 ± 1.0 eV is inaccurate. A better estimate of IE(ThC) can be established as 6.19 ± 0.34 eV using our value of $D_0(Th^+–C)$ along with $D_0(Th–C) = 4.70 \pm 0.18$ eV[53] in Eq. (1) (neglecting the difference between the 0 K and 298 K BDE).

Theoretical calculations establish $^2\Sigma^+$ ($1\sigma^2 1\pi^4 2\sigma$) as the ground state of ThC^+ where the 1σ is primarily the C 2*s*-orbital, the 1π orbitals are an interaction of the C 2*p*π and Th^+ 6*d*π-orbitals, and the 2σ is a bonding interaction between C 2*p*σ and a *sd*-hybridized Th^+ orbitals, consistent with the NBO analysis presented in Table S2. Thus, ThC^+ has a bond order of 2.5, explaining its weaker bond compared to ThO^+. A $^4\Pi$ excited state is found 0.52–0.94 eV higher in energy where one π-electron is moved to the 3σ-orbital (Th^+ 7*s*). A second excited state ($^2\Pi$) is found 0.55–0.86 eV higher than the ground state where one π-electron is moved to the 2σ-orbital. Other states found were at least 0.96 eV higher in energy than the ground state and are listed in Table II. Energies calculated using additional basis sets are listed in Table S1 in the supplementary material.[129]

B3LYP bond lengths for ThC^+ ground and excited states are listed in Table II and additional levels of theory are listed in Table S2. The calculated bond length is $r(Th^+–C) = 1.903$ Å, which is shorter than that calculated for $ThCH_2^+$,

r(Th^+–C) = 2.05 Å (B3LYP/SDD-VDZ-MWB), but similar to that for $ThCH^+$, 1.92 Å (B3LYP/SDD-VDZ-MWB).[16] These calculations also show that $ThCH^+$ has a triple bond, whereas $ThCH_2^+$ has a double bond, compared to the bond order for ThC^+ found here of 2.5. In our previous work, we also determined bond strengths of $D_0(Th^+–CH_2) \geq 4.54 \pm 0.09$ eV and $D_0(Th^+–CH) = 6.19 \pm 0.16$ eV. On the basis of the bond orders, one expects that $D_0(Th^+–C)$ should lie between these values, which is consistent with our 4.82 ± 0.29 eV BDE but inconsistent with the much lower 3.1 ± 1.0 eV.

Theoretical BDEs for ThC^+ are listed in Table IV. When including spin-orbit energy corrections, the BDEs are 4.84–5.21 eV (SDD-VDZ-MWB), 4.72–5.33 eV (Seg. SDD-VDZ-MWB), 4.81–5.20 eV (cc-pwCVQZ-PP), 4.99–5.38 eV (CBS-PP), and 5.00 eV (FPD). BDEs calculated with additional basis sets and methods are listed in Table S5 in the supplementary material.[129] In general, all levels of theory are in reasonable agreement with the experimental BDE. In particular, CCSD(T) (except non-composite CCSD(T)/CBS) values are within experimental uncertainty and B3LYP values are in excellent agreement with the experimental value. These values are similar to those calculated for $ThCH_2^+$, 4.44–5.04 eV (Seg. SDD-VQZ-MWB), and smaller than those reported for $ThCH^+$, 5.57–6.21 eV (Seg. SDD-VQZ-MWB).[16] This is again consistent with a bond order in between that of $ThCH_2^+$ (2) and $ThCH^+$ (3).

In order to calculate IE(ThC), additional calculations were performed for ThC using the B3LYP/cc-pwCVQZ-PP/aug-cc-pwCVQZ approach (as well as FPD). Additional single point energies were calculated using CCSD(T)/cc-pwCVQZ-PP/aug-cc-pwCVQZ with the B3LYP optimized structures. Results are listed in Table S6 in the supplementary material.[129] We find that the ThC ground state is $^3\Sigma^+$ ($1\sigma^2 1\pi^4 2\sigma 3\sigma$) where orbital compositions are similar to those of ThC^+ discussed above. Thus, the electron removed upon ionization of ThC is from the non-bonding 3σ (largely Th 7*s*) orbital so that it is likely that IE (ThC) ≈ IE(Th) and that $D_0(Th^+–C) \approx D_0$ (Th–C). Calculated ionization energies of ThC are 6.40 (B3LYP) and 6.33 (CCSD(T)) eV within experimental uncertainty of the 6.19 ± 0.34 eV value determined here and well below the electron impact values previously reported. The value of IE (ThC) obtained from the composite FPD approach is calculated to be 6.32 eV, whereas that of ThO is determined to be 6.60 eV. The former is well within the experimental uncertainty of the value determined experimentally here, while the FPD IE for ThO is in excellent agreement with the accurately known experimental value of 6.602 63 eV.[9]

POTENTIAL ENERGY SURFACES

$Th^+ + O_2$

Relaxed potential energy scans of the electronic surfaces for reaction (7), $Th^+ + O_2$, were calculated at the B3LYP/SDD-VDZ-MWB/6-311+G(3df) level and are presented in Figure 3. Notably, these surfaces (as well as those for $Th^+ + CO$) do not include consideration of spin-orbit effects. Initially, the reaction originates on a $^2A'$ surface where the minimum at very small angles can be understood as a linear Th^+–O–O

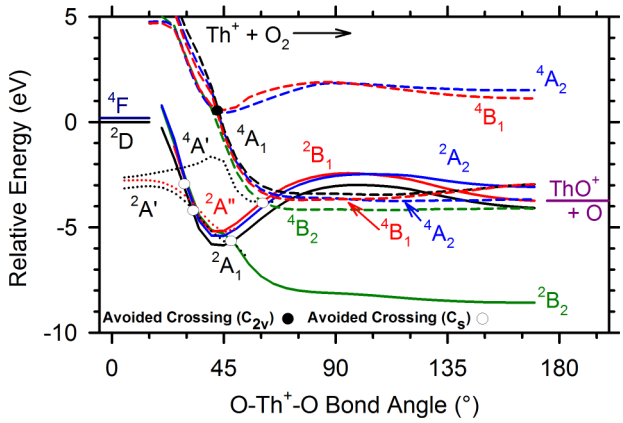

FIG. 3. B3LYP/SDD-VDZ-MWB/6-311+G(3df) relaxed potential energy surface calculations of the $Th^+ + O_2$ reaction as a function of ∠OTh$^+$O in degrees. Energies are relative to Th^+ (^2D, $6d7s^2$) + O_2. In C_{2v} symmetry, doublet surfaces are represented by solid lines and quartet surfaces by dashed lines. Surfaces with C_s symmetry are represented by dotted lines. No spin-orbit interactions are included.

intermediate that lies ~3 eV below the reactants. $^2A''$ and $^4A'$ surfaces lie slightly higher in energy. This $^2A'$ ($^2\Sigma^+$) intermediate has r(Th^+–O) = 1.92 Å, 0.11 Å longer than the 1.81 Å bond length in ThO^+ ($^2\Sigma^+$). The r(O–O) bond length of 1.32 Å is elongated from 1.20 Å in unbound O_2. The stability of these intermediates appears to come from a covalent interaction of the Th^+ 6*d*-electrons with the O_2 π^* antibonding electrons. At slightly larger angles, there is a slight barrier relative to the $^2A'$ intermediate along both doublet surfaces as Th^+ begins to insert into the O–O bond. At ~35°, there is an apparent crossing with the $^2A_1$, $^2A_2$, and $^2B_1$ surfaces that lead to potential wells near an angle of 45°. These are all still adducts of Th^+ with O_2, which pass over barriers as the ∠OThO angle increases, until dropping slightly as a linear thorium dioxide cation is approached. This leads to several excited states of linear ThO_2^+. The $^2A_1$ surface crosses that for the $^2B_2$ surface (avoided in C_S symmetry) which leads to a linear global minimum that is at least 3 eV lower in energy than all other surfaces and 8.5 eV below ground state reactants. This $^2B_2$ surface leads to the linear $^2\Sigma_u^+$ ground state of ThO_2^+, which has been previously characterized.[22] This intermediate should readily dissociate to the ThO^+ ($^2\Sigma^+$) + O (^3P) product asymptote, 4.8 eV higher in energy than ThO_2^+ ($^2\Sigma_u^+$). Clearly, these surfaces show that reaction (7) can occur with no barrier above the reactants on doublet surfaces, consistent with experiment. Further, the attractive nature of the surfaces is consistent with the efficiency of the reaction observed.

A number of quartet surfaces were also explored and are shown in Figure 3. These could also lead to the ThO^+ ($^2\Sigma^+$) + O (^3P) products with no barriers but are clearly higher energy pathways.

If spin-orbit effects are considered, the main change to the surface is the ground level of the reactants (and the principally occupied level) becomes Th^+ ($^4F_{3/2}$) + O_2 ($^3\Sigma_g^-$), which lies 0.40 eV lower than the ^2D state shown in Figure 3. These reactants can combine to form doublet, quartet, and sextet surfaces (where the latter should be largely repulsive as

they include no covalent interactions). Thus, evolution from reactants to products along the doublet (or quartet) surfaces remains barrierless and efficient.

$Th^+ + CO$

Surfaces from relaxed potential surface scans calculated using B3LYP/SDD-VDZ-MWB/6-311+G(3df) for reactions (9) and (10), $Th^+ + CO$, are presented in Figure 4. At small angles, the lowest energy reaction pathway evolves along the $^4A''$ surface where the initial intermediate is linear Th^+–C–O lying 1.4 eV below ground state reactants. A $^2A''$ state is also observed 1.2 eV below the reactants. Notably, at small angles near the reactant asymptote, s(s + 1) values for this $^2A''$ state are typically ~1.76, suggesting that there is considerable spin-contamination for this doublet surface. At slightly larger angles, barriers to Th^+ insertion into the C–O bond are observed. In this vicinity, a second $^4A''$ surface becomes the lowest energy surface and leads to an intermediate at 115°. This $^4A''$ intermediate has r(Th^+–O) = 1.82 Å, similar to the bond length of ThO^+, and r(Th^+–C) = 2.34 Å, which is significantly longer than the bond length of ThC^+. Thus, this intermediate can be viewed as an adduct between ThO^+ ($^2\Sigma^+$) and C (^{3}P), where the quartet spin indicates no covalent coupling between the two, such that this intermediate can readily dissociate to the ThO^+ ($^2\Sigma^+$) + C (^{3}P) asymptote 2.1 eV higher in energy than the reactant asymptote with no barrier above the product asymptote. Additionally, no barrier beyond the endothermicity of reaction (9) exists such that the global minimum can readily dissociate to the ThC^+ ($^2\Sigma^+$) + O (^{3}P) product asymptote that is ~6 eV higher in energy than the reactants. Overall, the potential energy surface (PES) in Figure 4 is very similar to the analogous $Hf^+ + CO$ reaction PES.[42] Like $Th^+ + CO$, Hf^+ has low-lying $^4A''$ and $^2A''$ surfaces that approach linear at small angles, and a $^4A''$ intermediate is found near 115°.

If spin-orbit effects are considered, the Th^+ ($^4F_{3/2}$) reacts with CO ($^1\Sigma^+$) along a quartet spin surface, however, because the J = 3/2 ground level is actually a mixture of $^4F_{3/2}$ and $^2D_{3/2}$, both doublet and quartet surfaces should be accessible in the reaction. Furthermore, this presumably permits switching between surfaces of different spin with some facility.

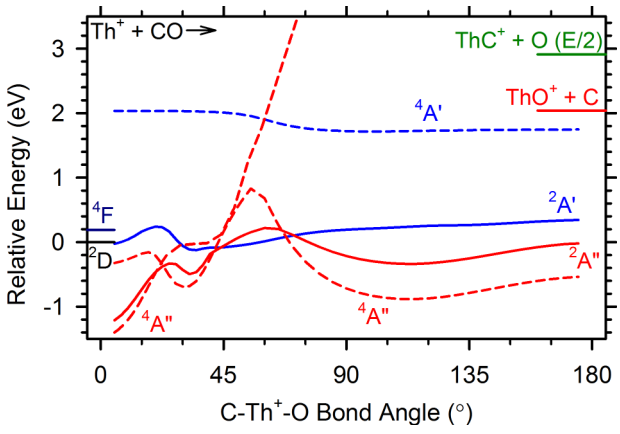

FIG. 4. B3LYP/SDD-VDZ-MWB/6-311+G(3df) relaxed potential energy surface calculations of the $Th^+ + CO$ reaction in C_s symmetry as a function of ∠CTh+O in degrees. Energies are relative to Th^+ (^{2}D, $6d7s^2$) + CO. Doublet surfaces are represented by solid lines and quartet surfaces by dashed lines. No spin-orbit interactions are included.

DISCUSSION

Composite thermochemical calculations

In previous calculations of actinide species,[72] the FPD composite approach without any higher-order correlation contributions reproduced the atomization energies of ThO and UF_n species within 0.05 eV of the mean experimental values. The present values calculated for ThO^+ and ThC^+ BDEs, which now include correlation contributions beyond just CCSD(T), are 8.68 and 5.00 eV, respectively, which are both within the experimental uncertainty of the experimental values presented here. The composite $D_0(Th^+–O)$ value also agrees very well with the values reported by Marçalo and Gibson[13] and Konings *et al.*[50] Interestingly, to confidently obtain an accuracy of a few kJ/mol as acquired here, CCSDTQ calculations are necessary (although the latter contributions were small relative to CCSDT, this was not known *a priori*). This is very similar to the situation for transition metal species (see, for instance, Ref. 128) and probably indicates that high level theoretical calculations are necessary to accurately reproduce experimental BDEs for actinide systems.

Assuming that the accuracy of the composite values is similar or higher to that previously reported, then the true values of $D_0(Th^+–O)$ and $D_0(Th^+–C)$ lie at the upper range of the uncertainty of the experimental values reported here. However, it must be noted that the estimates of the accuracy of the FPD composite approach for actinide systems are derived primarily from experimental values with stated uncertainties of 0.1–0.2 eV. Additional work, by both experiment and theory, is likely necessary to further evaluate the accuracy of the FPD composite approach for actinide thermochemical values but the present results are certainly promising.

Comparison of other theoretical methods

In past work,[16,17] we have compared values calculated using a number of theoretical methods and various basis sets to the experimentally determined thermochemistry of several ThL^+ species. Here we evaluate the performance of these methods and additional approaches in order to facilitate future computational work for Th and other actinide species.

Previously ThH^+ and $ThCH_3^+$ BDEs calculated utilizing CCSD(T)/cc-pVQZ-PP/cc-pVTZ yielded results that overestimated the experimental values by 0.2–0.6 eV, whereas the calculated BDE for $ThCH^+$ reproduced the experimental value reasonably well.[16] Here, CCSD(T)/cc-pwCVQZ-PP/aug-cc-pwCVQZ calculations overestimate the experimental BDE of ThO^+ and ThC^+ by 0.48 and 0.26 eV, respectively. Meanwhile, CCSD(T)/Seg. SDD-VQZ-MWB calculations reproduce the experimental value for both ThO^+ and ThC^+ within experimental uncertainty, and CCSD(T)/SDD-VDZ-MWB calculations reproduce the experimental ThC^+ BDE within uncertainty and overestimate the ThO^+ BDE by 0.25 eV. Mean absolute deviations (MADs) between the two experimental values and theory at the CCSD(T) level using cc-

pwCVQZ-PP, Seg. SDD-VQZ-MWB, and SDD-VDZ-MWB basis sets are 0.11, 0.06, and 0.14, respectively, indicating that, at least for calculating BDEs, there is no advantage in using the larger cc-pwCVQZ-PP basis set compared to the smaller Seg. SDD-VQZ-MWB basis set for these systems. Indeed, use of a complete basis set approach (CBS-PP) yields even worse results with a MAD of 0.36 eV. Similarly, MADs for these three basis sets using CCSD(T) are 0.28, 0.27, and 0.37, respectively, when comparing ThH^+, $ThCH^+$, $ThCH_3^+$, and $ThCH_4^+$ theoretical BDEs to experimental values. (Only a lower limit can be established for $ThCH_2^+$.)[16] As pointed out by a reviewer, this does not necessarily indicate that the smaller basis sets perform better, but rather may indicate that the valence electron only approach to the CCSD(T) calculation used here may be inadequate and that additional corrections may be needed.

For DFT methods, there is little difference between calculations using the cc-pwCVQZ-PP and Seg. SDD-VQZ-MWB basis sets for all methods, although the larger basis set yields values that average 0.09 ± 0.04 eV lower and closer to experiment. In general, these calculations generally overestimate the experimental BDE with the exception of BHLYP calculations. BHLYP has previously been shown to perform poorly for multiply bound species.[89] Calculations utilizing the SDD basis set also tend to overestimate the experimental BDEs, but with the exception of BHLYP calculations, perform better compared to the other two basis sets. MADs listed in Table IV indicate that there is little advantage to using the larger cc-pVQZ-PP and Seg. SDD basis sets in DFT calculations for these systems, with the latter basis set yielding the worst results.

In general, B3PW91 and PBE0 methods yield similar BDEs to each other regardless of the basis set used and tend to overestimate the experimental BDE with MADs of 0.29 and 0.28 eV, respectively (cc-pwCVQZ-PP). However, B3LYP calculations perform reasonably well with a MAD of 0.07 eV (0.14 and 0.03 eV for the Seg. SDD-VQZ-MWB and SDD-VDZ-MWB basis sets, respectively). In all calculations, the inclusion of spin-orbit effects improves accuracy compared to the experimental values. MADs comparing the lower order methods to the FPD values are similar to the MADs determined by comparing to experimental values.

In the present work, BHLYP/cc-pwCVQZ-PP calculations successfully predict the order and magnitude of the ThO^+ excited states, Table II. B3LYP/cc-pwCVQZ-PP and CCSD(T)/cc-pwCVQZ-PP perform similarly whereas the other methods predict the correct ordering but underestimate the energy gaps between excited states, Table II. In previous work,[16,17] BHLYP calculations reproduced the experimental order of Th^+ ground and excited states with a high degree of accuracy in the energy spacing whereas all other methods, including B3LYP and CCSD(T), either ordered the states incorrectly or spaced the states too closely. Although BHLYP performs poorly in predicting the absolute BDEs for higher bond order species, it appears to perform reasonably well at predicting relative energies of excited states.

Comparison to other metal oxide and carbide cations

One interesting aspect of Th^+ is that its ground level does not populate the $5f$-orbitals in the ground state, unlike the other members of the actinide series. Its J = 3/2 ground level configuration, a mixture of ^4F ($6d^27s$) and ^2D ($6d7s^2$), can be directly compared with those for the group 4 transition metal cations, Ti^+ (^4F, $3d^24s$), Zr^+ (^4F, $4d^25s$), and Hf^+ (^2D, $5d6s^2$), which also have three valence electrons. Such a comparison has profitably been included in our analysis of the $Th^+ + CH_4$[16] and $Th^+ + H_2$[17] systems, and others have noted the similarities in the electronic structures of Th^+ and Hf^+ species.[9,15] Here, we also include a comparison to the lanthanide Ce^+ (^4H, $4f5d^2$), which also has three valence electrons and is the lanthanide congener to actinide Th^+. With the exception of CeO^+, all thermochemical values in this discussion are measured from guided ion beam experiments.[38,40,42] A brief description of the thermochemical values used to evaluate $D_0(Ce^+–O)$ can be found in the supplementary material.[129]

MO^+ BDEs for the group 4 transition metals, Ce, and Th are listed in Table V in order of increasing atomic number. With the exception of HfO^+, the group 4 and Th^+ BDEs increase moving down the periodic table consistent with the trend expected for the lanthanide contraction where the $(n + 1)s$ orbital is preferentially stabilized compared to nd orbitals such that sd-hybridization is more efficient and leads to stronger σ-bonds.[89,130–132] The lower than expected BDE for Hf^+ is likely an electronic effect because the Hf^+ ground state (^2D, $5d6s^2$) has a doubly occupied $6s$ orbital that cannot readily form an $M^+–O$ triple bond, which requires the metal cation to have two unpaired electrons that can adopt π-symmetry.[133] Therefore, Hf^+ must be promoted to a higher state, thereby reducing the BDE. The first level with the correct symmetry ($^4F_{3/2}$, $5d^26s$) is 0.45 eV higher in energy than the ground level. Similarly, it might have been expected that $D_0(Th^+–O) > D_0(Ce^+–O)$, however, this discrepancy can potentially be explained by the considerable

TABLE V. Comparison of $D_0(M^+–L)$ bond dissociation energies (eV) for M = group 4, Ce, and Th and L = O and C.

L	$D_0(Ti^+–L)$[a]	$D_0(Zr^+–L)$[b]	$D_0(Ce^+–L)$	$D_0(Hf^+–L)$[c]	$D_0(Th^+–L)$
O	6.88 ± 0.07	7.76 ± 0.11	8.82 ± 0.21[d]	6.91 ± 0.11	8.57 ± 0.14
C	4.05 ± 0.24	4.72 ± 0.11	4.11 ± 0.82[e]	3.19 ± 0.03	4.82 ± 0.29

[a]Reference 38.
[b]Reference 40.
[c]Reference 42.
[d]This work, see supplementary material.[129]
[e]References 28 and 134.

^{2}D ($6d7s^2$) character mixed into the J = 3/2 ground level.[66] Furthermore, the lone electron in ThO^+, located in the 3σ nominally non-bonding orbital, may be pushed up in energy through configuration interaction with the 2σ-orbital, thereby weakening the overall bond energy. Such an interaction in CeO^+ is less likely to occur because the lone electron resides in a 4*f*-orbital that is decidedly non-bonding.

The periodic trends in the BDEs for MC^+ for the group 4 transition metal cations, CeC^+, and ThC^+ parallel the trends for MO^+. All MC^+ BDEs are listed in Table V and are taken from guided ion beam experiments except $D_0(Ce^+–C)$, which can be calculated using Eq. (1) from $D_0(Ce–C) = 4.57 \pm 0.12$ eV,[134] IE(CeC) = 6.0 ± 0.8 eV,[134] and IE(Ce) = 5.5387 eV[28] as $D_0(Ce^+–C) = 4.11 \pm 0.81$ eV. However, the large uncertainty makes comparison to the other metal cations inexact. Comparison with the oxide values suggests that the true CeC^+ BDE is close to the upper limit in this range.

With the exception of HfC^+, all BDEs increase moving down the periodic table consistent with the trend expected for the lanthanide contraction.[89,130–132] Like HfO^+, the lower than expected BDE for HfC^+ can be explained as a result of the Hf^+ ground state configuration (^{2}D, $5d6s^2$) that is not conducive to bonding.[42] This is largely supported by quantum chemical calculations that indicate that HfC^+ has a $^2\Sigma^+$ ($1\sigma^2 1\pi^4 2\sigma$) ground state that cannot be formed directly from the ground state Hf^+ (^{2}D, $6d7s^2$) + C (^{3}P, $2s^2 2p^2$) asymptote.

Another interesting aspect of the present results is the potential insight into the thermochemistry of other actinides that are more dangerous to work with experimentally. For comparison to the present work, we adopt the AnO^+ BDEs reported by Marçalo and Gibson[13] but note several potential discrepancies in the supplementary material.[129] BDEs are $D_0(Th^+–O) = 8.57 \pm 0.14$ eV > $D_0(Pa^+–O) = 8.29 \pm 0.52$ eV > $D_0(U^+–O) = 8.02 \pm 0.13$ eV > $D_0(Np^+–O) = 7.88 \pm 0.10$ eV > $D_0(Cm^+–O) = 6.94 \pm 0.39$ eV > $D_0(Pu^+–O) = 6.75 \pm 0.20$ eV > $D_0(Am^+–O) = 5.80 \pm 0.29$ eV. Gibson has previously shown[6] that this trend can be explained by a promotion energy argument where the AnO^+ BDE is lowered by the cost of promotion from the ground level to the first level with a $6d^2$ configuration. Thus an AnO^+ intrinsic BDE can be defined using[6]

$$D_0(An^+–O)^* = D_0(An^+–O) + E_p(6d^2). \quad (12)$$

Notably, because $E_p(Th^+) = 0$ eV, the ThO^+ BDE should act as a good estimate of the intrinsic actinide oxide cation BDE.

If the present value for $D_0(Th^+–O) = 8.57 \pm 0.14$ eV is used in Eq. (12) to predict $D_0(An^+–O)$, the predicted values have a MAD of 0.3 ± 0.3 eV compared to the experimental values. This offers no improvement over predictions obtained using Marçalo and Gibson's[13] proposed value of $D_0(Th^+–O) = 8.74 \pm 0.26$ eV in Eq. (12), where the MAD = 0.2 ± 0.2 eV. However, the comparison above of the ThO^+ BDE to group 4 transition metals and Ce^+ indicates that $D_0(Th^+–O)$ may be depressed by electronic effects, such that $E_p(Th^+) \neq 0$ eV, in which case $D_0(Th^+–O) = D_0(An^+–O)^*$ is not an exact approximation. Nevertheless, this model more accurately predicts $D_0(An^+–O)$ than reported DFT calculations where MADs of 0.7 ± 0.4 eV (B3LYP) and 0.6 ± 0.5 eV (MPW1PW91) are obtained.

Presumably a similar model to Eq. (12) can be used to explain AnC^+ BDE trends. However, unlike AnO^+ BDEs, the AnC^+ BDEs are unknown with the exception of ThC^+ reported here and $D_0(U^+–C) = 4.8 \pm 0.5$ eV derived from $D_0(U–C) = 4.72 \pm 0.16$ eV,[135] IE(UC) = 6.1 ± 0.5 eV,[136] and IE(U) = 6.1914 eV[28] utilizing Eq. (1). Assuming that $D_0(Th^+–C) = D_0(An^+–C)^*$ because $E_p(Th^+, 6d^2) = 0$ eV, one can estimate that $D_0(U^+–C) = D_0(Th^+ – C) – E_p(U^+, 6d^2) = 4.25 \pm 0.3$ eV given $E_p(U^+, 6d^2) = 0.57$ eV, which underestimates the experimental BDE of UC^+ but lies within the combined uncertainties.

CONCLUSION

Analysis of the kinetic energy dependence of the cross section from reaction (9), Figure 2, indicates that $D_0(Th^+–O) = 8.57 \pm 0.14$ eV. Although within experimental uncertainty of previously accepted literature values, the present value is ~0.2 eV lower, closely matching $D_0(Th^+–O) = 8.49 \pm 0.13$ and 8.59 ± 0.17 eV derived from Eq. (1) using the values originally reported by Hildenbrand and Murad[32] and Neubert and Zmbov,[34] respectively, coupled with updated IEs.[9,28] The discrepancy likely arises from the choice of parameters used to extrapolate data from high temperatures to 0 K for $D_0(Th–O)$, which can be a significant source of error as noted by Murad and Hildenbrand.[29,32] $D_0(Th^+–O)$ is larger than its transition metal cation congeners, Ti^+, Zr^+, and Hf^+, consistent with the result expected because of lanthanide contraction, however, $D_0(Th^+–O)$ is weaker than its lanthanide counterpart, $D_0(Ce^+–O)$, which can be explained in part by the mixed character of the Th^+ J = 3/2 ground level and by the apparent, slightly anti-bonding character of the 3σ (largely 7*s*) orbital (a result of configuration interaction) compared to the 4*f* non-bonding orbital in CeO^+.

Analysis of the cross section in reaction (10), Figure 2, provides the first experimental report of $D_0(Th^+–C) = 4.82 \pm 0.29$ eV. IE(ThC) = 6.19 ± 0.34 eV can also be calculated using Eq. (1) and the neutral ThC BDE reported by Gupta and Gingerich.[53] The ThC^+ BDE value agrees well with theoretical calculations and is a significant improvement over previous values reported on the basis of appearance energies in Knudsen effusion cell studies.[53] Like ThO^+, $D_0(Th^+–C)$ is larger than its transition metal cation congeners consistent with that expected because of lanthanide contraction.

In general, the approximate quantum chemical calculations overestimate the ThL^+ BDEs, but significant improvement is observed when including spin-orbit corrections using a semi-empirical approach. Using larger basis sets in coupled cluster calculations does not lead to any improvement in performance. This may be a result of the necessity of including higher order terms (i.e., CCSDT, CCSDT(Q), etc.) as demonstrated in composite chemistry calculations performed here. Indeed, FPD composite calculations lead to BDEs in good agreement with experimental values, suggesting that FPD represents an accurate approach to calculating actinide thermochemical values.

ACKNOWLEDGMENTS

This work is supported by the Heavy Element Chemistry Program, Office of Basic Energy Sciences, U.S. Department of Energy, through Grant Nos. DE-SC0012249 (P.B.A.) and DE-FG02-12ER16329 (K.A.P.). R.M.C. and P.B.A. also thank the Center for High Performance Computing at the University of Utah for the generous allocation of computer time. Dr. Bert de Jong is thanked for his helpful advice on spin-orbit calculations.

[1]P. B. Armentrout and J. L. Beauchamp, "Collision-induced dissociation of UO^+ and UO_2^+ ions," Chem. Phys. **50**(1), 21–25 (1980).
[2]P. B. Armentrout and J. L. Beauchamp, "Reactions of U^+ and UO^+ with O_2, CO, CO_2, OCS, CS_2 and D_2O," Chem. Phys. **50**(1), 27–36 (1980).
[3]H. H. Cornehl, R. Wesendrup, M. Diefenbach, and H. Schwarz, "A comparative study of oxo-ligand effects in the gas-phase chemistry of atomic lanthanide and actinide cations," Chem.–Eur. J. **3**(7), 1083–1090 (1997).
[4]J. K. Gibson and R. G. Haire, "Gas-phase chemistry of bare and oxo-ligated protactinium ions: A contribution to a systematic understanding of actinide chemistry," Inorg. Chem. **41**(22), 5897–5906 (2002).
[5]M. Santos, J. Marçalo, A. P. de Matos, J. K. Gibson, and R. G. Haire, "Gas-phase oxidation reactions of neptunium and plutonium ions investigated via Fourier transform ion cyclotron resonance mass spectrometry," J. Phys. Chem. A **106**(31), 7190–7194 (2002).
[6]J. K. Gibson, "Role of atomic electronics in f-element bond formation: Bond energies of lanthanide and actinide oxide molecules," J. Phys. Chem. A **107**(39), 7891–7899 (2003).
[7]M. Santos, J. Marçalo, J. P. Leal, A. P. de Matos, J. K. Gibson, and R. G. Haire, "FTICR-MS study of the gas-phase thermochemistry of americium oxides," Int. J. Mass Spectrom. **228**(2-3), 457–465 (2003).
[8]J. K. Gibson, R. G. Haire, M. Santos, J. Marçalo, and A. P. de Matos, "Oxidation studies of dipositive actinide ions, An^{2+} (An = Th, U, Np, Pu, Am) in the gas phase: Synthesis and characterization of the isolated uranyl, neptunyl, and plutonyl ions UO_2^{2+}(g), NpO_2^{2+}(g), and PuO_2^{2+} (g)," J. Phys. Chem. A **109**(12), 2768–2781 (2005).
[9]V. Goncharov and M. C. Heaven, "Spectroscopy of the ground and low-lying excited states of ThO^+," J. Chem. Phys. **124**(6), 064312 (2006).
[10]M. C. Heaven, "Probing actinide electronic structure using fluorescence and multi-photon ionization spectroscopy," Phys. Chem. Chem. Phys. **8**(39), 4497–4509 (2006).
[11]J. K. Gibson, R. G. Haire, J. Marçalo, M. Santos, J. P. Leal, A. P. de Matos, R. Tyagi, M. K. Mrozik, R. M. Pitzer, and B. E. Bursten, "FTICR/MS studies of gas-phase actinide ion reactions: Fundamental chemical and physical properties of atomic and molecular actinide ions and neutrals," Eur. Phys. J. D **45**(1), 133–138 (2007).
[12]J. K. Gibson, R. G. Haire, J. Marçalo, M. Santos, A. P. de Matos, M. K. Mrozik, R. M. Pitzer, and B. E. Bursten, "Gas-phase reactions of hydrocarbons with An^+ and AnO^+ (An = Th, Pa, U, Np, Pu, Am, Cm): The active role of 5f electrons in organoprotactinium chemistry," Organometallics **26**(16), 3947–3956 (2007).
[13]J. Marçalo and J. K. Gibson, "Gas-phase energetics of actinide oxides: An assessment of neutral and cationic monoxides and dioxides from thorium to curium," J. Phys. Chem. A **113**(45), 12599–12606 (2009).
[14]C. C. L. Pereira, C. J. Marsden, J. Marçalo, and J. K. Gibson, "Actinide sulfides in the gas phase: Experimental and theoretical studies of the thermochemistry of AnS (An = Ac, Th, Pa, U, Np, Pu, Am and Cm)," Phys. Chem. Chem. Phys. **13**(28), 12940–12958 (2011).
[15]M. C. Heaven, B. J. Barker, and I. O. Antonov, "Spectroscopy and structure of the simplest actinide bonds," J. Phys. Chem. A **118**(46), 10867–10881 (2014).
[16]R. M. Cox, P. B. Armentrout, and W. A. de Jong, "Activation of CH_4 by Th^+ as studied by guided ion beam mass spectrometry and quantum chemistry," Inorg. Chem. **54**(7), 3584–3599 (2015).
[17]R. M. Cox, P. B. Armentrout, and W. A. de Jong, "Reactions of $Th^+ + H_2$, D_2, and HD studied by guided ion beam tandem mass spectrometry and quantum chemical calculations," J. Phys. Chem. B **120**, 1601–1614 (2016).
[18]G. Mazzone, M. d. C. Michelini, N. Russo, and E. Sicilia, "Mechanistic aspects of the reaction of Th^+ and Th^{2+} with water in the gas phase," Inorg. Chem. **47**(6), 2083–2088 (2008).
[19]K. J. de Almeida and H. A. Duarte, "Gas-phase methane activation by the Ac^+– Pu^+ Ions: Theoretical insights into the role of 5f electrons/orbitals in early actinide chemistry," Organometallics **28**, 3203–3211 (2009).
[20]E. di Santo, M. d. C. Michelini, and N. Russo, "Methane C–H bond activation by gas-phase Th^+ and U^+: Reaction mechanisms and bonding analysis," Organometallics **28**(13), 3716–3726 (2009).
[21]E. di Santo, M. C. Michelini, and N. Russo, "Activation of ethane C–H and C–C bonds by gas phase Th^+ and U^+: A theoretical study," J. Phys. Chem. A **113**(52), 14699–14705 (2009).
[22]I. Infante, A. Kovacs, M. G. La, A. R. M. Shahi, J. K. Gibson, and L. Gagliardi, "Ionization energies for the actinide Mono- and dioxides series, from Th to Cm: Theory versus experiment," J. Phys. Chem. A **114**(19), 6007–6015 (2010).
[23]J. Zhou and H. B. Schlegel, "*Ab initio* molecular dynamics study of the reaction between Th^+ and H_2O," J. Phys. Chem. A **114**(33), 8613–8617 (2010).
[24]K. J. de Almeida and H. A. Duarte, "Dehydrogenation of methane by gas-phase Th, Th^+, and Th^{2+}: Theoretical insights into actinide chemistry," Organometallics **29**, 3735–3745 (2010).
[25]A. Kovacs and R. J. M. Konings, "Computed vibrational frequencies of actinide oxides $AnO^{0/+/2+}$ and $AnO_2^{0/+/2+}$ (An = Th, Pa, U, Np, Pu, Am, Cm)," J. Phys. Chem. A **115**(24), 6646–6656 (2011).
[26]B. B. Averkiev, M. Mantina, R. Valero, I. Infante, A. Kovacs, D. G. Truhlar, and L. Gagliardi, "How accurate are electronic structure methods for actinoid chemistry?," Theor. Chem. Acc. **129**(3-5), 657–666 (2011).
[27]S. Kohler, R. Deissenberger, K. Eberhardt, N. Erdmann, G. Herrmann, G. Huber, J. V. Kratz, M. Nunnemann, G. Passler, P. M. Rao, J. Riegel, N. Trautmann, and K. Wendt, "Determination of the first ionization potential of actinide elements by resonance ionization mass spectroscopy," Spectrochim. Acta, Part B **52**(6), 717–726 (1997).
[28]J. E. Sansonetti and W. C. Martin, "Handbook of basic atomic spectroscopic data," J. Phys. Chem. Ref. Data **34**(4), 1559–2259 (2005).
[29]J. B. Pedley and E. M. Marshall, "Thermochemical data for gaseous monoxides," J. Phys. Chem. Ref. Data **12**(4), 967–1031 (1983).
[30]R. J. Ackermann, E. G. Rauh, R. J. Thorn, and M. C. Cannon, "A thermodynamic study of the thorium-oxygen system at high temperatures," J. Phys. Chem. **67**, 762–769 (1963).
[31]R. J. Ackermann and E. G. Rauh, "High-temperature properties of the thorium-oxygen system. Revision of the thermodynamic properties of thorium(II) oxide (g) and thorium(IV) oxide (g)," High Temp. Sci. **5**(6), 463–473 (1973).
[32]D. L. Hildenbrand and E. Murad, "Mass spectrometric studies of gaseous thorium monoxide and thorium dioxide," J. Chem. Phys. **61**(3), 1232–1237 (1974).
[33]E. Murad and D. L. Hildenbrand, "Thermochemical properties of gaseous zirconium(II) oxide and zirconium(IV) oxide," J. Chem. Phys. **63**(3), 1133–1139 (1975).
[34]A. Neubert and K. F. Zmbov, "Mass spectrometric determination of the dissociation energy of the thorium oxide molecule," High Temp. Sci. **6**(4), 303–308 (1974).
[35]S. K. Loh, L. Lian, and P. B. Armentrout, "Oxidation reactions at variably sized transition metal Centers: Iron and niobium ions + molecular oxygen (Fe_n^+ and $Nb_n^+ + O_2$ (n = 1-3))," J. Chem. Phys. **91**(10), 6148–6163 (1989).
[36]S. K. Loh, E. R. Fisher, L. Lian, R. H. Schultz, and P. B. Armentrout, "State-specific reactions of Fe^+ (^6D, ^4F) with oxygen and oxirane: $D_0(Fe^+–O)$ and effects of collisional relaxation," J. Phys. Chem. **93**(8), 3159–3167 (1989).
[37]E. R. Fisher, J. L. Elkind, D. E. Clemmer, R. Georgiadis, S. K. Loh, N. Aristov, L. S. Sunderlin, and P. B. Armentrout, "Reactions of fourth-period metal ions (Ca^+–Zn^+) with O_2: Metal–oxide ion bond energies," J. Chem. Phys. **93**(4), 2676–2691 (1990).
[38]D. E. Clemmer, J. L. Elkind, N. Aristov, and P. B. Armentrout, "Reactions of Sc^+, Ti^+, and V^+ with CO. MC^+ and MO^+ bond energies," J. Chem. Phys. **95**(5), 3387–3393 (1991).
[39]Y.-M. Chen and P. B. Armentrout, "Kinetic energy dependence of the reactions of Ru^+, Rh^+, Pd^+, and Ag^+ with O_2," J. Chem. Phys. **103**(2), 618–625 (1995).
[40]M. R. Sievers, Y.-M. Chen, and P. B. Armentrout, "Metal oxide and carbide thermochemistry of Y^+, Zr^+, Nb^+, and Mo^+," J. Chem. Phys. **105**(15), 6322–6333 (1996).
[41]X.-G. Zhang and P. B. Armentrout, "Activation of O_2, CO, and CO_2 by Pt^+: The thermochemistry of PtO^+," J. Phys. Chem. A **107**(42), 8904–8914 (2003).
[42]C. S. Hinton, F. Li, and P. B. Armentrout, "Reactions of Hf^+, Ta^+, and W^+ with O_2 and CO: Metal carbide and metal oxide cation bond energies," Int. J. Mass Spectrom. **280**(1-3), 226–234 (2009).
[43]P. B. Armentrout, "The bond energy of ReO^+: Guided ion-beam and theoretical studies of the reaction of Re^+ (^7S) with O_2," J. Chem. Phys. **139**, 084305 (2013).

[44]P. B. Armentrout and F.-X. Li, "Bond energy of IrO^+: Guided ion-beam and theoretical studies of the reaction of Ir^+ (^5F) with O_2," J. Phys. Chem. A **117**(33), 7754–7766 (2013).

[45]G. Edvinsson, PhD dissertation, USIP Report 71-09, Stockholm, 1971.

[46]K. P. Huber and G. Herzberg, "Constants of diatomic molecules," in *NIST Chemistry WebBook, NIST Standard Reference 69*, edited by P. J. Linstrom and W. G. Mallard (National Institute of Standards and Technology, Gaithersburg, MD, 20899), http://webbook.nist.gov (retrieved March 2016).

[47]J. Paulovic, T. Nakajima, K. Hirao, R. Lindh, and P. A. Malmqvist, "Relativistic and correlated calculations on the ground and excited states of ThO," J. Chem. Phys. **119**(2), 798–805 (2003).

[48]W. Kuechle, M. Dolg, H. Stoll, and H. Preuss, "Energy-adjusted pseudopotentials for the actinides. Parameter sets and test calculations for thorium and thorium monoxide," J. Chem. Phys. **100**(10), 7535–7542 (1994).

[49]S. G. Lias, J. E. Bartmess, J. F. Liebman, J. L. Holmes, R. D. Levin, and W. G. Mallard, "Gas-phase ion and neutral thermochemistry," J. Phys. Chem. Ref. Data, Suppl. **17**(1), 1–861 (1988).

[50]R. J. M. Konings, O. Benes, A. Kovacs, D. Manara, D. Sedmidubsky, L. Gorokhov, V. S. Iorish, V. Yungman, E. Shenyavskaya, and E. Osina, "The thermodynamic properties of the f-elements and their compounds. II. The lanthanide and actinide oxides," J. Phys. Chem. Ref. Data **43**(1), 01310101–01310195 (2014).

[51]J. Sugar, "Revised ionization energies of the neutral actinides," J. Chem. Phys. **60**(10), 4103 (1974).

[52]E. G. Rauh and R. J. Ackermann, "First ionization potentials of some refractory oxide vapors," J. Chem. Phys. **60**(4), 1396–1400 (1974).

[53]S. K. Gupta and K. A. Gingerich, "A thermodynamic study of the gaseous thorium carbides, ThC, ThC_2, ThC_3, ThC_4, ThC_5, and ThC_6," J. Chem. Phys. **72**(4), 2795–2800 (1980).

[54]F. J. Kohl and C. A. Stearns, "Vaporization and dissociation energies of the molecular carbides of titanium, zirconium, hafnium, and thorium," High Temp. Sci. **6**(4), 284–302 (1974).

[55]S. K. Loh, D. A. Hales, L. Li, and P. B. Armentrout, "Collision-induced dissociation of iron cluster ions (Fe_n^+) (n = 2-10) with xenon: Ionic and neutral iron binding energies," J. Chem. Phys. **90**(10), 5466–5485 (1989).

[56]R. H. Schultz and P. B. Armentrout, "Reactions of nitrogen ion (N_4^+) with rare gases from thermal to 10 eV center-of-mass energy: Collision-induced dissociation, charge transfer and ligand exchange," Int. J. Mass Spectrom. Ion Processes **107**(1), 29–48 (1991).

[57]E. Teloy and D. Gerlich, "Integral cross sections for ion-molecule reactions. I. Guide beam technique," Chem. Phys. **4**(3), 417–427 (1974).

[58]P. B. Armentrout, "Kinetic energy dependence of ion-molecule reactions: Guided ion beams and threshold measurements," Int. J. Mass Spectrom. **200**(1/3), 219–241 (2000).

[59]K. M. Ervin and P. B. Armentrout, "Translational energy dependence of $Ar^+ + XY \rightarrow ArX^+ + Y$ (XY = H_2,D_2,HD) from thermal to 30 eV c.m.," J. Chem. Phys. **83**(1), 166–189 (1985).

[60]P. J. Chantry, "Doppler broadening in beam experiments," J. Chem. Phys. **55**(6), 2746–2759 (1971).

[61]C. L. Haynes and P. B. Armentrout, "Thermochemistry and structures of $CoC_3H_6^+$: Metallacycle and metal-alkene isomers," Organometallics **13**(9), 3480–3490 (1994).

[62]D. E. Clemmer, Y.-M. Chen, F. A. Khan, and P. B. Armentrout, "State-specific reactions of Fe^+(a^6D, a^4F) with D_2O and reactions of FeO^+ with D_2," J. Phys. Chem. **98**, 6522–6529 (1994).

[63]B. L. Kickel and P. B. Armentrout, "Reactions of Fe^+, Co^+, and Ni^+ with silane. Electronic state effects, comparison to reactions with methane, and M^+–SiHx (x = 0-3) bond energies," J. Am. Chem. Soc. **117**(2), 764–773 (1995).

[64]B. L. Kickel and P. B. Armentrout, "Guided ion beam studies of the reactions of group 3 metal ions (Sc^+, Y^+, La^+, and Lu^+) with silane. Electronic state effects, comparison to reactions with methane, and M^+–SiHx (x = 0-3) bond energies," J. Am. Chem. Soc. **117**(14), 4057–4070 (1995).

[65]M. R. Sievers, Y.-M. Chen, J. L. Elkind, and P. B. Armentrout, "Reactions of Y^+, Zr^+, Nb^+, and Mo^+ with H_2, HD, and D_2," J. Phys. Chem. **100**(1), 54–62 (1996).

[66]J. Blaise and J.-F. Wyart, "Selected Constants, energy levels and atomic spectra of actinides," http://web2.lac.u-psud.fr/lac/Database/Contents.html (accessed 2 September 2015).

[67]W. J. Chesnavich and M. T. Bowers, "Theory of translationally driven reactions," J. Phys. Chem. **83**(8), 900–905 (1979).

[68]F. Muntean and P. B. Armentrout, "Guided ion beam study of collision-induced dissociation dynamics: Integral and differential cross sections," J. Chem. Phys. **115**(3), 1213–1228 (2001).

[69]N. Aristov and P. B. Armentrout, "Reaction mechanisms and thermochemistry of $V^+ + C_2H_{2p}$ (p = 1,2,3)," J. Am. Chem. Soc. **108**, 1806–1819 (1986).

[70]M. E. Weber, J. L. Elkind, and P. B. Armentrout, "Kinetic energy dependence of $Al^+ + O_2 \rightarrow AlO^+ + O$," J. Chem. Phys. **84**(3), 1521–1529 (1986).

[71]M. J. Frisch, G. W. Trucks, H. B. Schlegel, G. E. Scuseria, M. A. Robb, J. R. Cheeseman, G. Scalmani, V. Barone, B. Mennucci, G. A. Petersson, H. Nakatsuji, M. Caricato, X. Li, H. P. Hratchian, A. F. Izmaylov, J. Bloino, G. Zheng, J. L. Sonnenberg, M. Hada, M. Ehara, K. Toyota, R. Fukuda, J. Hasegawa, M. Ishida, T. Nakajima, Y. Honda, O. Kitao, H. Nakai, T. Vreven, J. A. Montgomery, Jr., J. E. Peralta, F. Ogliaro, M. Bearpark, J. J. Heyd, E. Brothers, K. N. Kudin, V. N. Staroverov, R. Kobayashi, J. Normand, K. Raghavachari, A. Rendell, J. C. Burant, S. S. Iyengar, J. Tomasi, M. Cossi, N. Rega, N. J. Millam, M. Klene, J. E. Knox, J. B. Cross, V. Bakken, C. Adamo, J. Jaramillo, R. Gomperts, R. E. Stratmann, O. Yazyev, A. J. Austin, R. Cammi, C. Pomelli, J. W. Ochterski, R. L. Martin, K. Morokuma, V. G. Zakrzewski, G. A. Voth, P. Salvador, J. J. Dannenberg, S. Dapprich, A. D. Daniels, Ö. Farkas, J. B. Foresman, J. V. Ortiz, J. Cioslowski, and D. J. Fox, Gaussian 09, Revision A.1, Gaussian Inc., Wallingford, CT, 2009.

[72]K. A. Peterson, "Correlation consistent basis sets for actinides. I. The Th and U atoms," J. Chem. Phys. **142**(7), 074105 (2015).

[73]A. Weigand, X. Cao, T. Hangele, and M. Dolg, "Relativistic small-core pseudopotentials for actinium, thorium, and protactinium," J. Phys. Chem. A **118**(13), 2519–2530 (2014).

[74]X. Cao, M. Dolg, and H. Stoll, "Valence basis sets for relativistic energy-consistent small-core actinide pseudopotentials," J. Chem. Phys. **118**(2), 487–496 (2003).

[75]D. E. Woon and T. H. Dunning, Jr., "Gaussian basis sets for use in correlated molecular calculations. V. Core-valence basis sets for boron through neon," J. Chem. Phys. **103**(11), 4572–4585 (1995).

[76]T. H. Dunning, Jr., "Gaussian basis sets for use in correlated molecular calculations. I. The atoms boron through neon and hydrogen," J. Chem. Phys. **90**(2), 1007–1023 (1989).

[77]R. Krishnan, J. S. Binkley, R. Seeger, and J. A. Pople, "Self-consistent molecular orbital methods. XX. A basis set for correlated wave functions," J. Chem. Phys. **72**(1), 650–654 (1980).

[78]A. Karton and J. M. L. Martin, "Comment on: "Estimating the Hartree-Fock limit from finite basis set calculations" [Jensen, F., Theor. Chem. Acc. 113, 267 (2005)]," Theor. Chem. Acc. **115**(4), 330–333 (2006).

[79]J. M. L. Martin, "*Ab initio* total atomization energies of small molecules–towards the basis set limit," Chem. Phys. Lett. **259**(5,6), 669–678 (1996).

[80]L. Andrews, Y. Gong, B. Liang, V. E. Jackson, R. Flamerich, S. Li, and D. A. Dixon, "Matrix infrared spectra and theoretical studies of thorium oxide species: ThO_x and Th_2O_y," J. Phys. Chem. A **115**, 14407–14416 (2011).

[81]L. Andrews, K. S. Thanthiriwatte, X. Wang, and D. A. Dixon, "Thorium fluorides ThF, ThF_2, ThF_3, ThF_4, $ThF_3(F_2)$, and ThF_5– characterized by infrared spectra in solid argon and electronic structure and vibrational frequency calculations," Inorg. Chem. **52**, 8228–8233 (2013).

[82]K. S. Thanthiriwatte, X. Wang, L. Andrews, D. A. Dixon, J. Metzger, T. Vent-Schmidt, and S. Riegel, "Properties of ThF_x from infrared spectra in solid argon and neon with supporting electronic structure and thermochemical calculations," J. Phys. Chem. A **118**, 2107–2119 (2014).

[83]A. D. Becke, "Density-functional thermochemistry. III. The role of exact exchange," J. Chem. Phys. **98**(7), 5648–5652 (1993).

[84]C. Lee, W. Yang, and R. G. Parr, "Development of the Colle-Salvetti correlation-energy formula into a functional of the electron density," Phys. Rev. B: Condens. Matter **37**(2), 785–789 (1988).

[85]J. P. Perdew, K. Burke, and Y. Wang, "Generalized gradient approximation for the exchange-correlation hole of a many-electron system," Phys. Rev. B: Condens. Matter **54**(23), 16533–16539 (1996).

[86]A. D. Becke, "A new mixing of Hartree-Fock and local-density-functional theories," J. Chem. Phys. **98**(2), 1372–1377 (1993).

[87]Y. Zhao and D. G. Truhlar, "The M06 suite of density functionals for main group thermochemistry, thermochemical kinetics, noncovalent interactions, excited states, and transition elements: Two new functionals and systematic testing of four M06-class functionals and 12 other functionals," Theor. Chem. Acc. **120**(1-3), 215–241 (2008).

[88]C. Adamo and V. Barone, "Toward reliable density functional methods without adjustable parameters: The PBE0 model," J. Chem. Phys. **110**(13), 6158–6170 (1999).

[89]X. Zhang and H. Schwarz, "Bonding in cationic MCH_2^+ (M = K–La, Hf–Rn): A theoretical study on periodic trends," Chem.–Eur. J. **16**, 5882–5888 (2010).

[90]G. D. Purvis III and R. J. Bartlett, "A full coupled-cluster singles and doubles model: The inclusion of disconnected triples," J. Chem. Phys. **76**(4), 1910–1918 (1982).
[91]J. A. Pople, M. Head-Gordon, and K. Raghavachari, "Quadratic configuration interaction. A general technique for determining electron correlation energies," J. Chem. Phys. **87**(10), 5968–5975 (1987).
[92]G. E. Scuseria, C. L. Janssen, and H. F. Schaefer III, "An efficient reformulation of the closed-shell coupled cluster single and double excitation (CCSD) equations," J. Chem. Phys. **89**(12), 7382–7387 (1988).
[93]G. E. Scuseria and H. F. Schaefer III, "Is coupled cluster singles and doubles (CCSD) more computationally intensive than quadratic configuration interaction (QCISD)?," J. Chem. Phys. **90**(7), 3700–3703 (1989).
[94]J. B. Foresman and A. E. Frisch, *Exploring Chemistry with Electronic Structure Methods*, 2nd ed. (Gaussian, Inc., Pittsburgh, PA, 1996).
[95]M. A. Garcia and M. D. Morse, "Resonant two-photon ionization spectroscopy of jet-cooled OsN: 520–418 nm," J. Chem. Phys. **135**, 114304 (2011).
[96]P. B. Armentrout, L. Parke, C. Hinton, and M. Citir, "Activation of methane by Os+: Guided-ion-beam and theoretical studies," ChemPlusChem **78**(9), 1157–1173 (2013).
[97]D. Feller, K. A. Peterson, and D. A. Dixon, "A survey of factors contributing to accurate theoretical predictions of atomization energies and molecular structures," J. Chem. Phys. **129**(20), 204105 (2008).
[98]M. Vasiliu, K. A. Peterson, J. K. Gibson, and D. A. Dixon, "Reliable potential energy surfaces for the reactions of H_2O with ThO_2, PaO_2^+, UO_2^{2+}, and UO_2^+," J. Phys. Chem. A **119**(46), 11422–11431 (2015).
[99]M. Douglas and N. M. Kroll, "Quantum electrodynamical corrections to the fine structure of helium," Ann. Phys. (N. Y.) **82**(1), 89–155 (1974).
[100]M. Reiher and A. Wolf, "Exact decoupling of the dirac Hamiltonian. II. The generalized Douglas-Kroll-Hess transformation up to arbitrary order," J. Chem. Phys. **121**(22), 10945–10956 (2004).
[101]R. A. Kendall, T. H. Dunning, Jr., and R. J. Harrison, "Electron affinities of the first-row atoms revisited. Systematic basis sets and wave functions," J. Chem. Phys. **96**(9), 6796–6806 (1992).
[102]W. A. de Jong, R. J. Harrison, and D. A. Dixon, "Parallel Douglas-Kroll energy and gradients in NWChem: Estimating scalar relativistic effects using Douglas-Kroll contracted basis sets," J. Chem. Phys. **114**(1), 48–53 (2001).
[103]K. A. Peterson and T. H. Dunning, Jr., "Accurate correlation consistent basis sets for molecular core–valence correlation effects: The second row atoms Al–Ar, and the first row atoms B–Ne revisited," J. Chem. Phys. **117**, 10548 (2002).
[104]G. E. Scuseria, "The open-shell restricted Hartree-Fock singles and doubles coupled-cluster method including triple excitations CCSD(T): Application to the carbon triatomic monopositive ion," Chem. Phys. Lett. **176**(1), 27–35 (1991).
[105]J. D. Watts, J. Gauss, and R. J. Bartlett, "Coupled-cluster methods with noniterative triple excitations for restricted-open-shell-Hartree-Fock and other general single-determinant reference functions. Energies and analytical gradients," J. Chem. Phys. **98**(11), 8718–8733 (1993).
[106]P. J. Knowles, C. Hampel, and H. J. Werner, "Coupled cluster theory for high spin, open shell reference wave functions," J. Chem. Phys. **99**(7), 5219–5227 (1993).
[107]H.-J. Werner, P. J. Knowles, G. Knizia, F. R. Manby, M. Schutz, P. Celani, T. Korona, R. Lindh, A. Mitrushenkov, G. Rauhut, K. R. Shamasundar, T. B. Adler, R. D. Amos, A. Bernhardsson, A. Berning, D. L. Cooper, M. J. O. Deegan, A. J. Dobbyn, F. Eckert, E. Goll, C. Hampel, A. Hesselmann, G. Hertzer, T. Hrenar, G. Jansen, C. Koppl, Y. Liu, A. W. Lloyd, R. A. Mata, A. J. May, S. J. McNicholas, W. Meyer, M. E. Mura, A. Nicklass, D. P. O'Neill, P. Palmieri, D. Peng, K. Pflüger, R. Pitzer, M. Reiher, T. Shiozaki, H. Stoll, A. J. Stone, R. Tarroni, T. Thorsteinsson, and M. Wang, MOLPRO, version 2012.1, a package of *ab initio* programs, 2012, see http://www.molpro.net.
[108]Y.-C. Park, I. S. Lim, and Y. S. Lee, Bull. Korean Chem. Soc. **33**, 803 (2012).
[109]L. Visscher, T. J. Lee, and K. G. Dyall, "Formulation and implementation of a relativistic unrestricted coupled-cluster method including noniterative connected triples," J. Chem. Phys. **105**(19), 8769–8776 (1996).
[110]L. Visscher, E. Eliav, and U. Kaldor, "Formulation and implementation of the relativistic Fock-space coupled cluster method for molecules," J. Chem. Phys. **115**, 9720–9726 (2001).
[111]R. Bast, T. Saue, L. Visscher, H. J. Aa. Jensen, V. Bakken, K. G. Dyall, S. Dubillard, U. Ekstroem, E. Eliav, T. Enevoldsen, E. Fasshauer, T. Fleig, O. Fossgaard, A. S. P. Gomes, T. Helgaker, J. Henriksson, M. Ilias, Ch. R. Jacob, S. Knecht, S. Komorovsky, O. Kullie, J. K. Laerdahl, C. V. Larsen, Y. S. Lee, H. S. Nataraj, M. K. Nayak, P. Norman, G. Olejniczak, J. Olsen, Y. C. Park, J. K. Pedersen, M. Pernpointner, R. Di Remigio, K. Ruud, P. Salek, B. Schimmelpfennig, J. Sikkema, A. J. Thorvaldsen, J. Thyssen, J. van Stralen, S. Villaume, O. Visser, T. Winther, and S. Yamamoto, DIRAC, a relativistic ab initio electronic structure program, Release DIRAC15 (2015) (see http://www.diracprogram.org).
[112]C. E. Moore, "Atomic energy levels," in *NSRDS-NBS* (Office of Standard Reference Data, National Bureau of Standards, Washington, DC, 1971), Vol. 35.
[113]K. G. Dyall, C. W. Bauschlicher, D. W. Schwenke, and P. Pyykko, "Is the lamb shift chemically significant?," Chem. Phys. Lett. **348**(5,6), 497–500 (2001).
[114]P. Pyykko and L.-B. Zhao, "Search for effective local model potentials for simulation of quantum electrodynamic effects in relativistic calculations," J. Phys. B: At., Mol. Opt. Phys. **36**(8), 1469–1478 (2003).
[115]J. Noga and R. J. Bartlett, "The full CCSDT model for molecular electronic structure," J. Chem. Phys. **86**(12), 7041–7050 (1987).
[116]G. E. Scuseria and H. F. Schaefer III, "A new implementation of the full CCSDT model for molecular electronic structure," Chem. Phys. Lett. **152**(4-5), 382–386 (1988).
[117]J. D. Watts and R. J. Bartlett, "The coupled-cluster single, double, and triple excitation model for open-shell single reference functions," J. Chem. Phys. **93**(8), 6104–6105 (1990).
[118]S. A. Kucharski and R. J. Bartlett, "Recursive intermediate factorization and complete computational linearization of the coupled-cluster single, double, triple, and quadruple excitation equations," Theor. Chim. Acta **80**(4-5), 387–405 (1991).
[119]N. Oliphant and L. Adamowicz, "Multireference coupled-cluster method using a single-reference formalism," J. Chem. Phys. **94**(2), 1229–1235 (1991).
[120]S. A. Kucharski and R. J. Bartlett, "The coupled-cluster single, double, triple, and quadruple excitation method," J. Chem. Phys. **97**(6), 4282–4288 (1992).
[121]M. Kallay and P. R. Surjan, "Higher excitations in coupled-cluster theory," J. Chem. Phys. **115**(7), 2945–2954 (2001).
[122]A. MRCC, *String-Based Quantum Chemical Program Suite* (University of Technology and Economics, Budapest, 2001).
[123]G. Gioumousis and D. P. Stevenson, "Reactions of gaseous molecule ions with gaseous molecules. V. Theory," J. Chem. Phys. **29**, 294–299 (1958).
[124]NIST Computational Chemistry Comparison and Benchmark Database NIST Standard Reference Database Number 101 Release 16a, http://cccbdb.nist.gov (accessed 20 August 2014).
[125]J. T. Waber and D. T. Cromer, "Orbital radii of atoms and ions," J. Chem. Phys. **42**(12), 4116–4123 (1965).
[126]K. P. Huber and G. Herzberg, *Molecular Spectra and Molecular Structure. IV. Constants of Diatomic Molecules* (Van Nostrand Reinhold Co., 1979).
[127]R. M. Cox and P. B. Armentrout (to be published).
[128]D. H. Bross, J. G. Hill, H. J. Werner, and K. A. Peterson, "Explicitly correlated composite thermochemistry of transition metal species," J. Chem. Phys. **139**, 094302 (2013).
[129]See supplementary material at http://dx.doi.org/10.1063/1.4948812 for analysis of the coupling between V_4 and V_1 potential energy surfaces. Brief evaluation of CeO^+ literature values. ThL^+ (L = C,O) BDEs and molecular parameters of the ground and excited states evaluated at additional levels of theory. Quantum chemical calculations of ThC.
[130]X.-G. Zhang, R. Liyanage, and P. B. Armentrout, "The potential energy surface for activation of methane by Pt^+: A detailed guided-ion beam study," J. Am. Chem. Soc. **123**, 5563–5575 (2001).
[131]X.-G. Zhang and P. B. Armentrout, "Reactions of Pt^+ with H_2, D_2, and HD: Effect of lanthanide contraction on reactivity and thermochemistry," J. Chem. Phys. **116**(13), 5565–5573 (2002).
[132]F.-X. Li, X.-G. Zhang, and P. B. Armentrout, "The most reactive third-row transition metal: Guided ion beam and theoretical studies of the activation of methane by Ir^+," Int. J. Mass Spectrom. **255/256**, 279–300 (2006).
[133]D. Schroder, H. Schwarz, and S. Shaik, "Characterization, orbital description, and reactivity patterns of transition-metal oxo species in the gas phase," Struct. Bonding (Berlin) **97**, 91–123 (2000).
[134]J. E. Kingcade, Jr., D. L. Cocke, and K. A. Gingerich, "Thermodynamic stabilities of the gaseous cerium carbides CeC, CeC_2, CeC_3, CeC_4, CeC_5, and CeC_6," High Temp. Sci. **16**(2), 89–109 (1983).
[135]S. K. Gupta and K. A. Gingerich, "Observations and atomization energies of the gaseous uranium carbides, UC, UC_2, UC_3, UC_4, UC_5, and UC_6 by high-temperature mass spectrometry," J. Chem. Phys. **71**(7), 3072–3080 (1979).
[136]K. A. Gingerich, "Mass-spectrometric evidence for the molecules uranium carbide and ceric carbide and predicted stability of diatomic carbides of electropositive transition metals," J. Chem. Phys. **50**(5), 2255–2256 (1969).